Phases and Entanglement in Neutron Interference Experiments

S. Filipp, J. Klepp, H. Lemmel, S. Sponar
Y. Hasegawa, H. Rauch

Atominstitut der Österreichischen Universitäten

Outline

- Neutron Interferometry Basics
  - Interferometry
  - Polarimetry
  - UCNMR
- Phases
  - Confinement induced phase
  - Geometric Phase (spin, spatial, mixed, stability)
  - Dephasing
- Spin-Path Entanglement
  - State Tomography
  - Bell Inequality Test - Quantum Contextuality

Neutron Interferometry

Self interference of massive particle (phase space density $\approx 10^{-14}$)

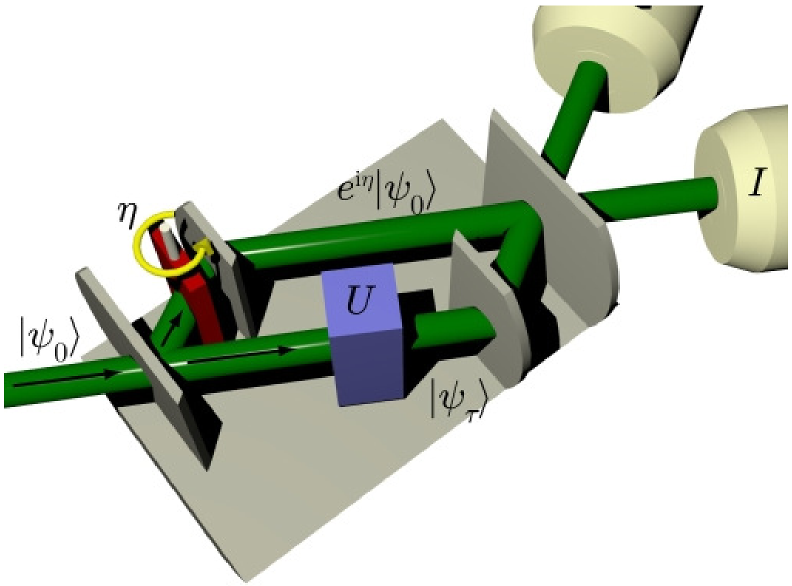

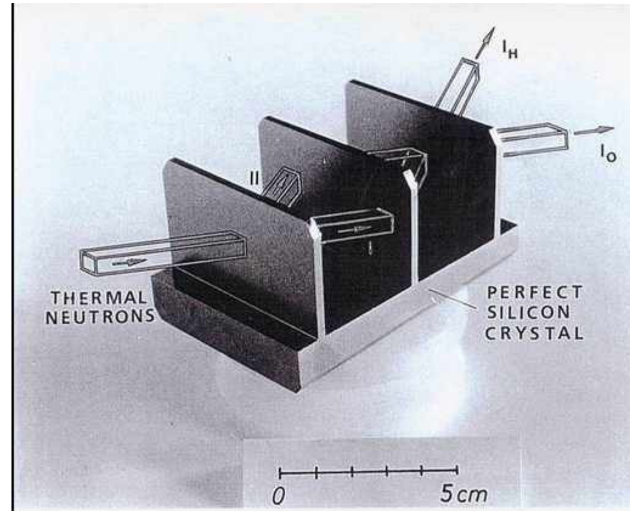

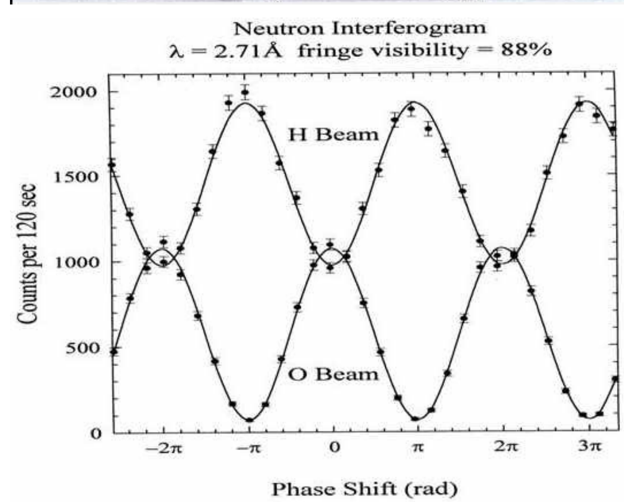

H. Rauch, W. Treimer and U. Bonse, PLA **47** 369 (1974).

Neutron Interferometry

- Time-Independent Schrödinger Equation: $\frac{\hbar^2}{2m}\left[\Delta+\frac{2m}{\hbar^2}\left(E-V(\vec{r})\right)\right]\psi(\vec{r})=0$

ATOMINSTITUT FWF

Neutron Interferometry

- Time-Independent Schrödinger Equation: $\frac{\hbar^2}{2m}\left[\Delta + \frac{2m}{\hbar^2}\left(E - V(\vec{r})\right)\right]\psi(\vec{r}) = 0$
- Wavefunction: $\psi(\vec{r}) = \frac{1}{(2\pi)^{3/2}}\int a(\vec{k})e^{i\vec{k}\cdot\vec{r}}d^3k \otimes \psi_{spin}$

ATOMINSTITUT FWF

Neutron Interferometry

- Time-Independent Schrödinger Equation: $\frac{\hbar^2}{2m}\left[\Delta + \frac{2m}{\hbar^2}\left(E - V(\vec{r})\right)\right]\psi(\vec{r}) = 0$
- Wavefunction: $\psi(\vec{r}) = \frac{1}{(2\pi)^{3/2}}\int a(\vec{k})e^{i\vec{k}\cdot\vec{r}}d^3k \otimes \psi_{spin}$
- Typical Potentials $V(\vec{r})$:
  - Scalar Fermi Potential (Nuclear Interaction): $V_N(\vec{r}) = \frac{2\pi\hbar^2}{m}b_c N$
    $\rightarrow$ phase shift $|\psi\rangle \mapsto e^{iNb_c\lambda D}|\psi\rangle$
  - Vector Potential (Magnetic interaction): $V_M(\vec{r}) = -\vec{\mu}_n \cdot \vec{B}$
    $\rightarrow$ Spinor rotation $|\psi_{spin}\rangle \mapsto U|\psi_{spin}\rangle, \quad (U = e^{-i\frac{\omega_L t}{2}\vec{\sigma}_n} \in SU(2))$

Neutron Interferometry

- Time-Independent Schrödinger Equation: $\frac{\hbar^2}{2m}\left[\Delta + \frac{2m}{\hbar^2}\left(E - V(\vec{r})\right)\right]\psi(\vec{r}) = 0$
- Wavefunction: $\psi(\vec{r}) = \frac{1}{(2\pi)^{3/2}}\int a(\vec{k})e^{i\vec{k}\cdot\vec{r}}d^3k \otimes \psi_{spin}$
- Typical Potentials $V(\vec{r})$:
  - Scalar Fermi Potential (Nuclear Interaction): $V_N(\vec{r}) = \frac{2\pi\hbar^2}{m}b_c N$
    $\rightarrow$ phase shift $|\psi\rangle \mapsto e^{iNb_c\lambda D}|\psi\rangle$
  - Vector Potential (Magnetic interaction): $V_M(\vec{r}) = -\vec{\mu}_n \cdot \vec{B}$
    $\rightarrow$ Spinor rotation $|\psi_{spin}\rangle \mapsto U|\psi_{spin}\rangle, \quad (U = e^{-i\frac{\omega_L t}{2}\vec{\sigma}_n} \in SU(2))$

$$I = \frac{1}{2}|\psi_\tau + e^{i\eta}\psi_0|^2$$
$$= 1 + \underbrace{|\psi_0^*\psi_\tau|}_{\nu}\cos(\eta - \underbrace{\arg\psi_0^*\psi_\tau}_{\Phi})$$

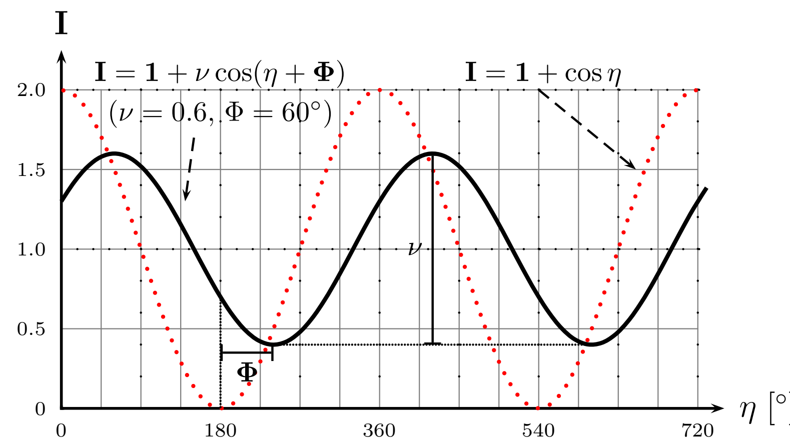

H. Rauch and S. A. Werner, *Neutron Interferometry* Clarendon Press, Oxford (2000).

Polarimetry

- Spin superposition, instead of different paths ($|+x\rangle = \frac{1}{\sqrt{2}}(|+z\rangle + |-z\rangle)$)
- $\frac{\pi}{2}$-flip $\widehat{=}$ beamsplitter
- Phase is encoded in the final polarization

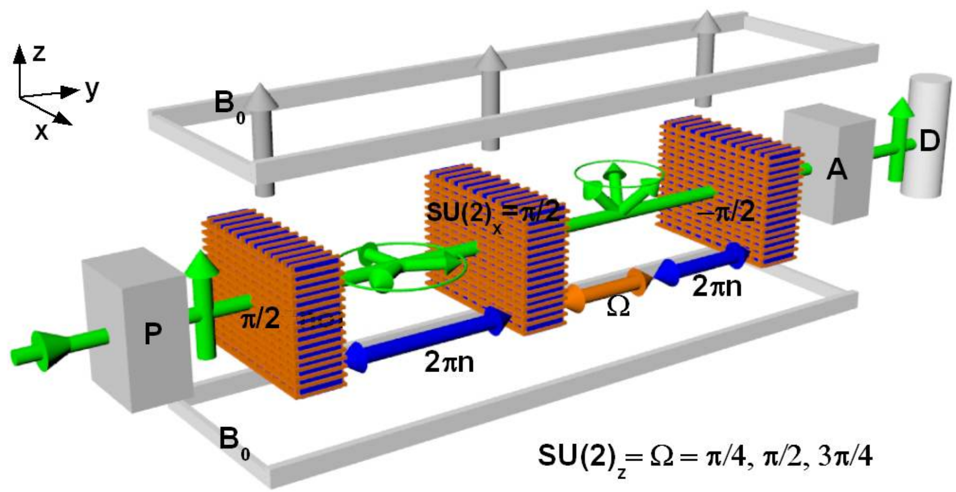

Intensity: $\boxed{I = \left|\, \langle +z|\, \hat{U}_{\text{out}}^{-\pi/2}\, \hat{U}_{L'}^{2n\pi-\eta}\, \hat{U}_0(\xi,\delta,\zeta)\, \hat{U}_L^{\eta}\, \hat{U}_{\text{in}}^{\pi/2}|+z\rangle\, \right|^2}$

Measured phase: $\boxed{\phi \equiv \arg\langle\psi_0|\psi\rangle = \arg\langle +z|\hat{U}_0|+z\rangle}$

UCNMR

- polarized Ultra Cold Neutrons (UCN's)
- low velocity $\approx 5m/s$ $(10^{-7}eV)$
- Fermi potential e. g. $2 \times 10^{-7}eV$ for stainless steel
- reflection at material wall
- neutron bottle
- wrap coils around for magnetic field
- polarimetric measurement

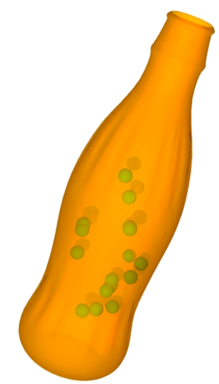

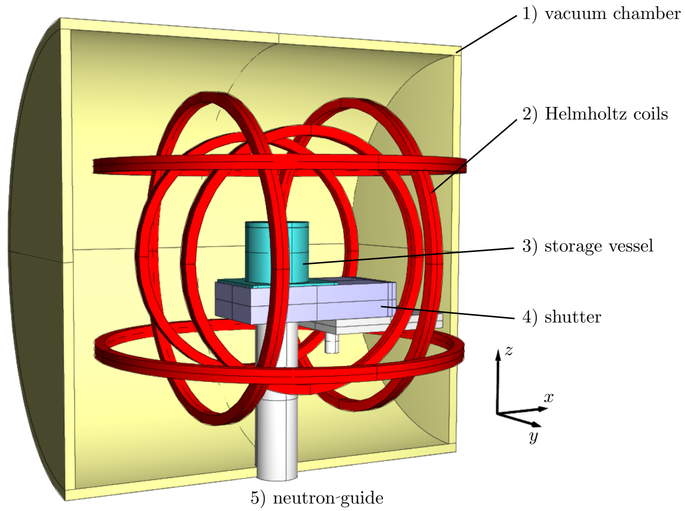

Confinement Induced Phase Shift

H. Rauch and H. Lemmel. Measurement of a confinement induced neutron phase. Nature **417**, 630-632 (2002)

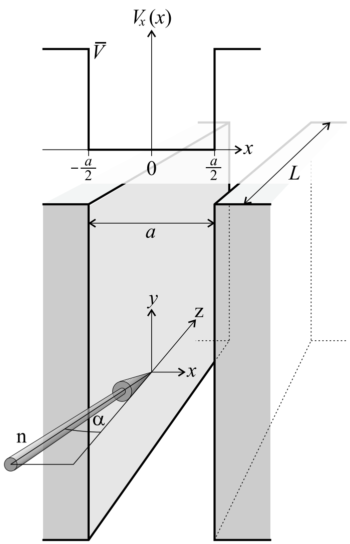

- transverse confinement
- discrete transverse energy levels
- increase of transverse momentum
- decrease of longitudinal momentum
  $\rightarrow$ phase shift

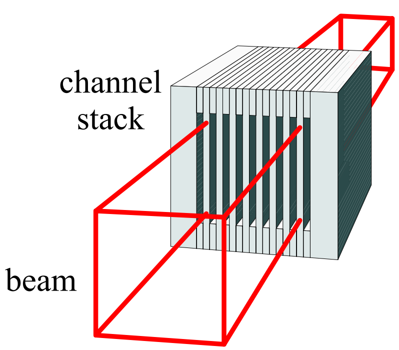

neutron wavelength	$\lambda = 1.86 \cdot 10^{-10}$m
neutron energy	$E = 0.023$eV
level energies	$E_n = 0.42, 1.7, 3.7, ...$peV
wall potential	$V_0 = Nb_c 2\pi\hbar^2/m \approx 54$neV
wall material	silicon
channel width	$a = 20\mu$m
channel length	$L = 2$cm
number of channels	≈ 250

J.
M. Lévy-Leblond. Phys. Lett. A **125**, 441-442 (1987); D. M. Greenberger, Physica B **151**, 374-377 (1988)

Measured phase shift

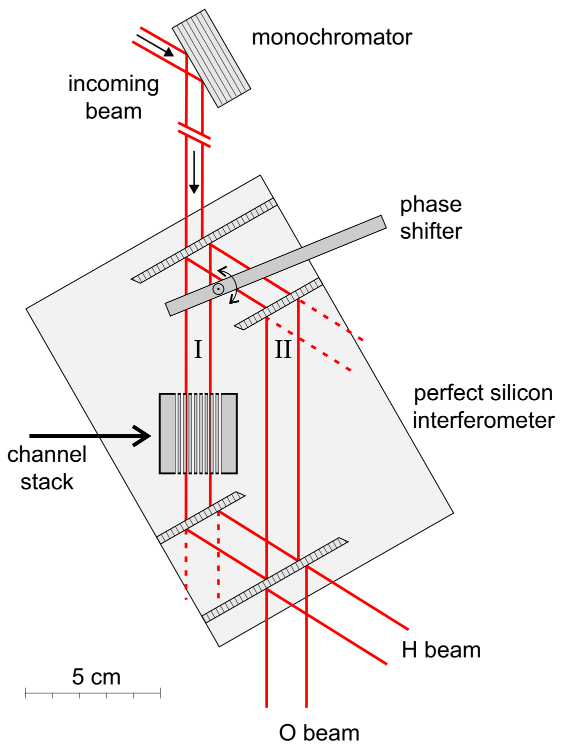

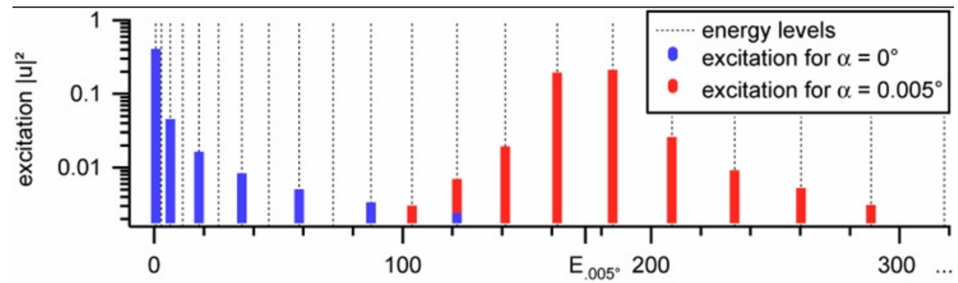

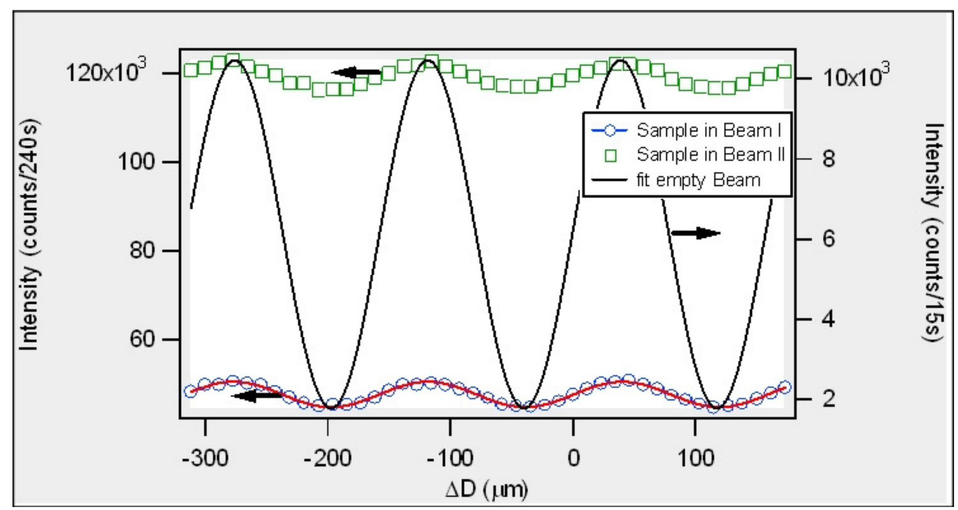

Calculated Phase Shift: $\Delta\phi = 2.5°$

Measured Phase Shift: $\Delta\phi = 2.8(4)°$

From falling cats...

A falling cat always lands on its feet.

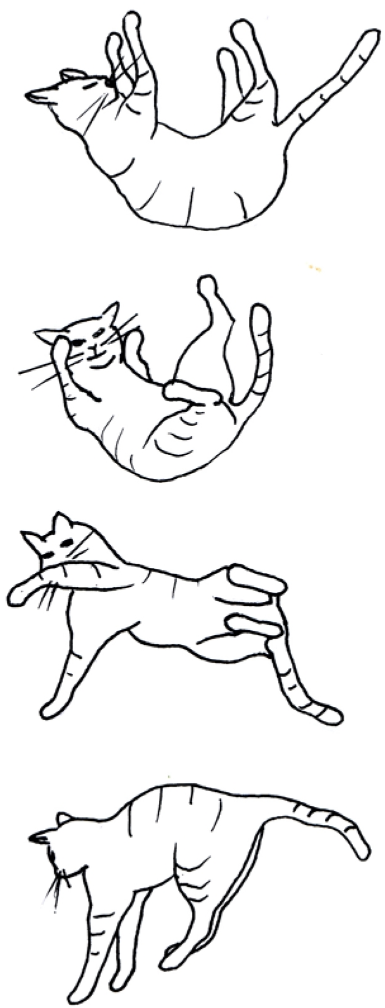

R. Montgomery, Commun. Math. Phys. **128**, 565 (1990).

...to Quantum Geometric Phases

Adiabatic, Cyclic Evolution of eigen-states

Berry phase

[Proc. R. S. Lond. A **392, 45 (1984)**]

$$H(R(t))|n(R(t))\rangle = E_n(t)|n(R(t))\rangle$$

$$\begin{aligned} |\psi(\tau)\rangle &= e^{-i\phi_d} e^{i\phi_g(C)} |n(R(\tau))\rangle \\ \phi_d(\tau) &= \frac{1}{\hbar}\int_0^\tau dt E_n(t) \\ \phi_g(C) &= \oint dR \cdot \langle n(R)|\nabla_R|n(R)\rangle \end{aligned}$$

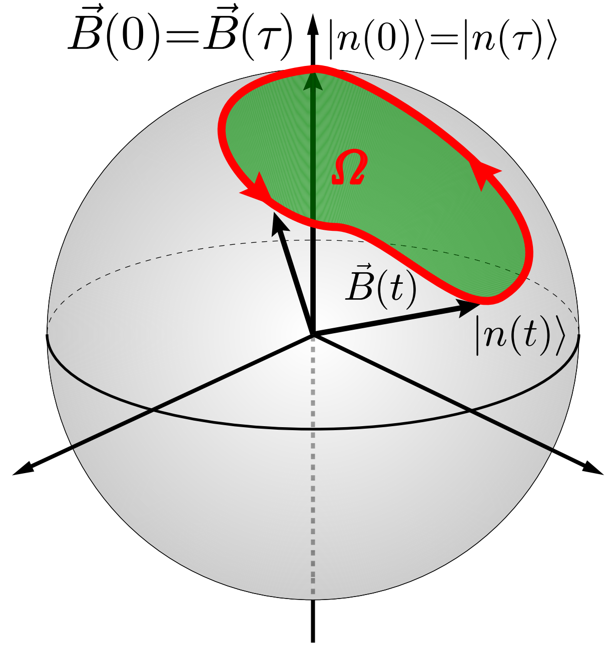

$$\boxed{\phi_g = -\frac{\Omega}{2}}$$

Geometric Phase in a Neutron Interferometer

- Spin-Flipper in one path rotates spin about axis $\vec{n}$ in x-y-plane
- Direction of axis depends on the phase

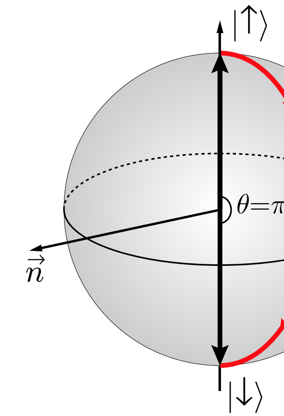

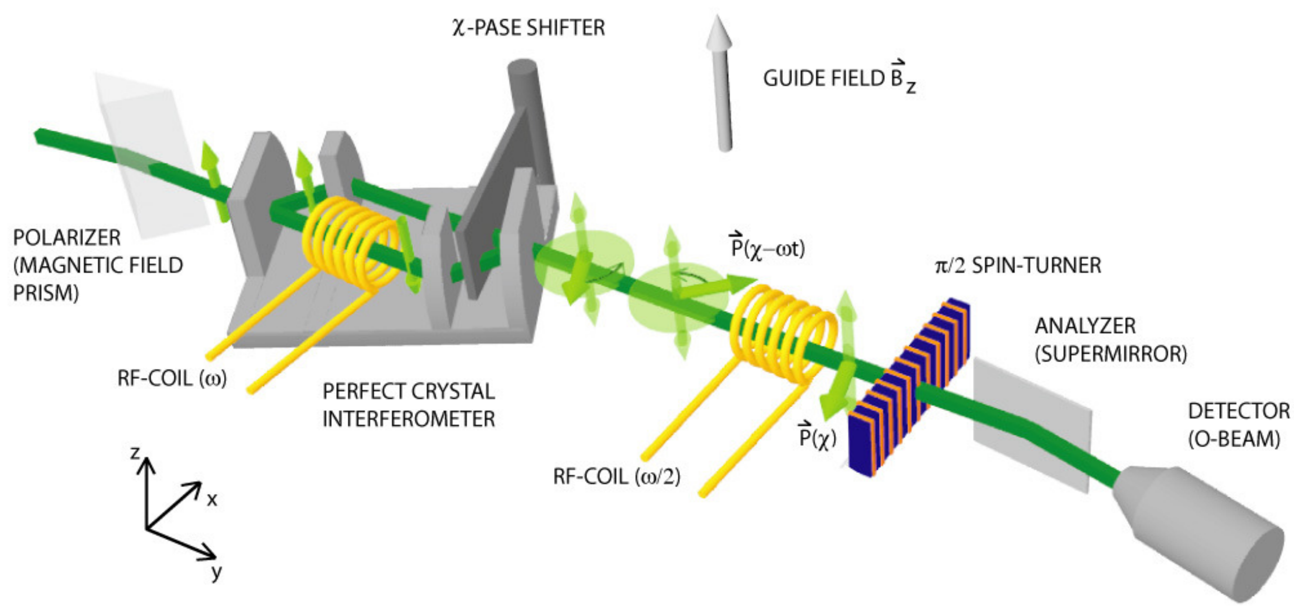

Geometric Phase in a Neutron Interferometer

- Spin-Flipper in one path rotates spin about axis $\vec{n}$ in x-y-plane
- Direction of axis depends on the phase
- In addition: Photon exchange $\hbar\omega = 2\mu B$

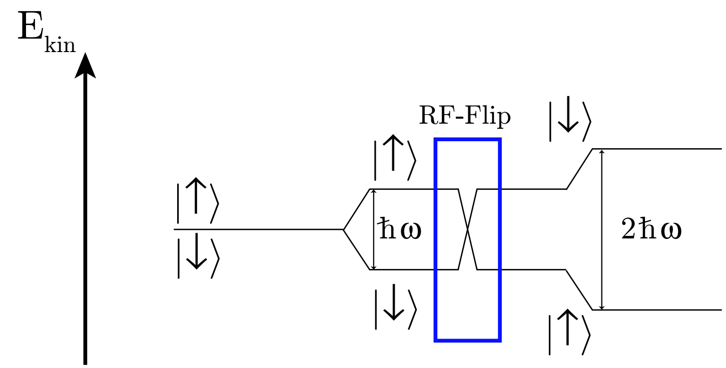

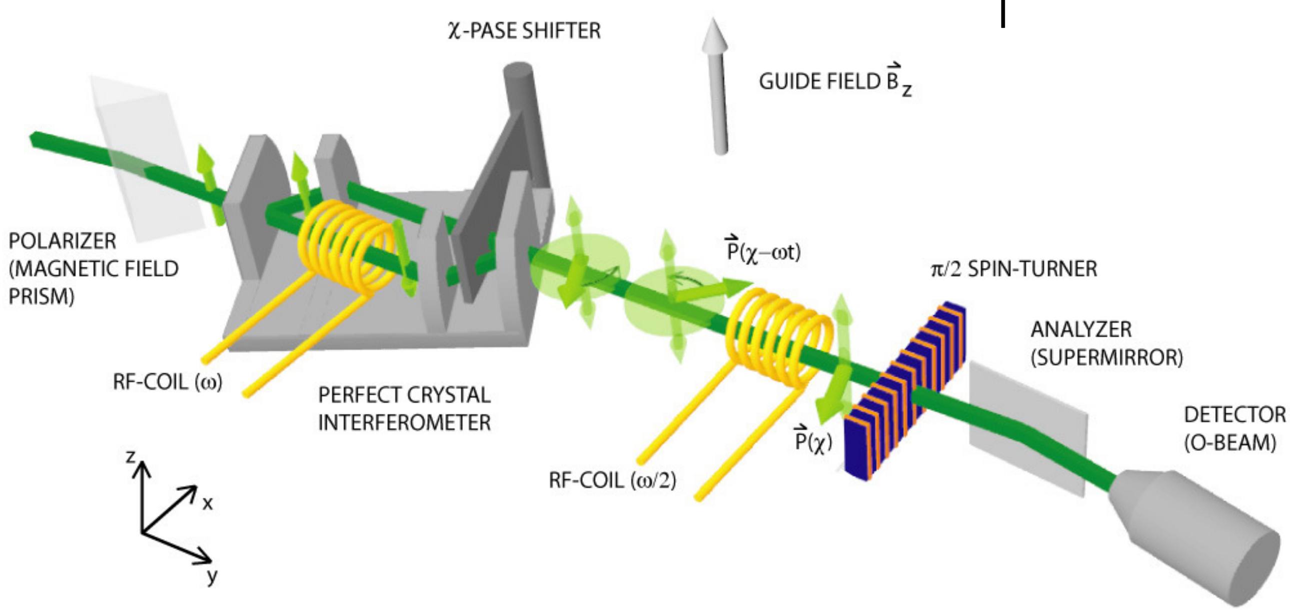

Geometric Phase in a Neutron Interferometer

- Spin-Flipper in one path rotates spin about axis $\vec{n}$ in x-y-plane
- Direction of axis depends on the phase
- In addition: Photon exchange $\hbar\omega = 2\mu B$
- 1^{st} spin flipper: $\sin\omega t$; 2^{nd} spin flipper: $\sin(\frac{\omega t}{2} + \phi)$
- Different frequencies: Compensation of different energies

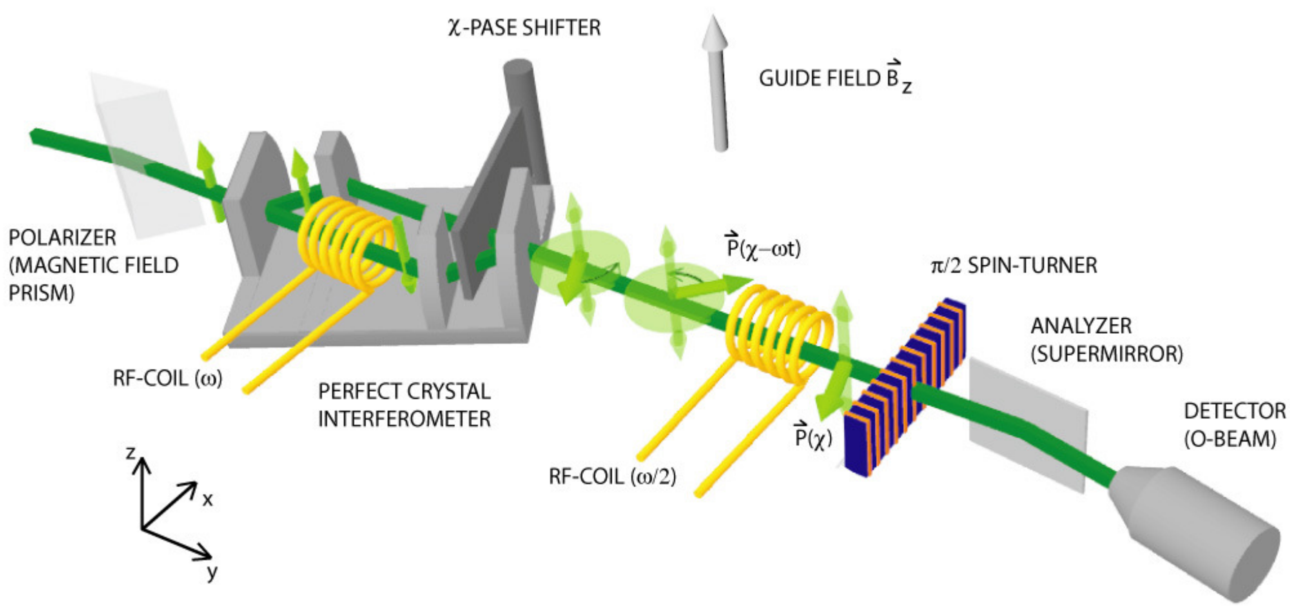

Orange-slice geometric phase

Alltogether: “Orange-slice” shaped path → geometric phase

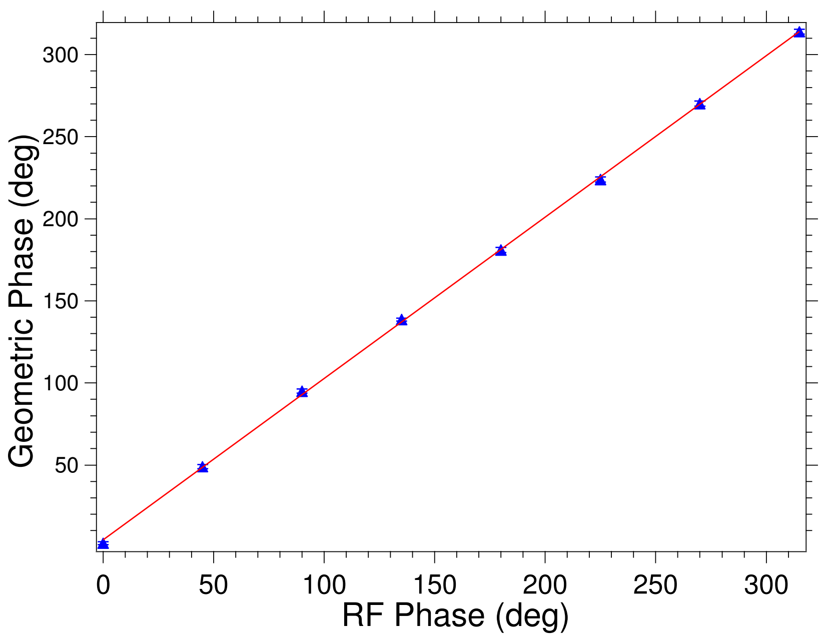

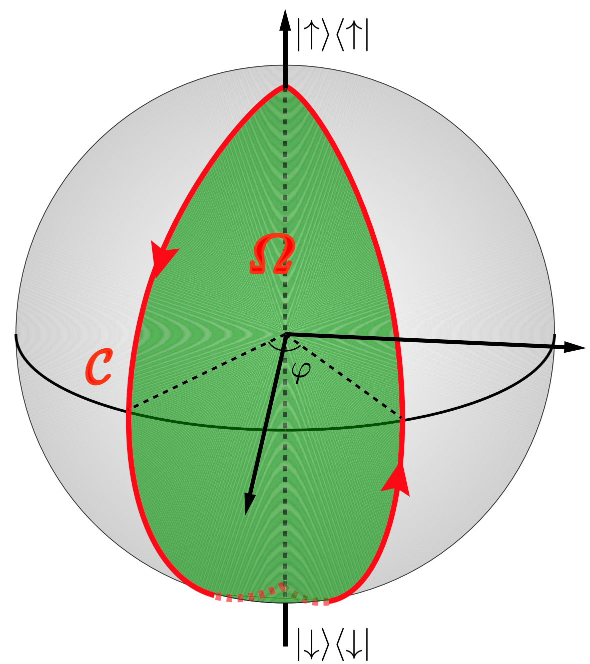

S. Sponar, J. Klepp, R. Loidl, S. Filipp and Y. Hasegawa (in preparation).

Spatial geometric phase

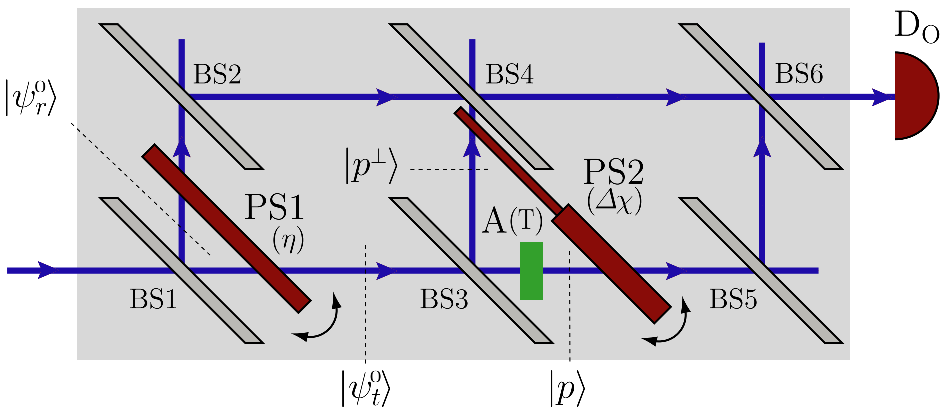

- 2-loop interferometer, unpolarized neutrons
- Geometric phase due to spatial degrees of freedom (2-level system)
- Phase Shifts $e^{i\chi_1}$, $e^{i\chi_2}$; Aborber (Transmission T)

ATOMINSTITUT FWF

Spatial geometric phase

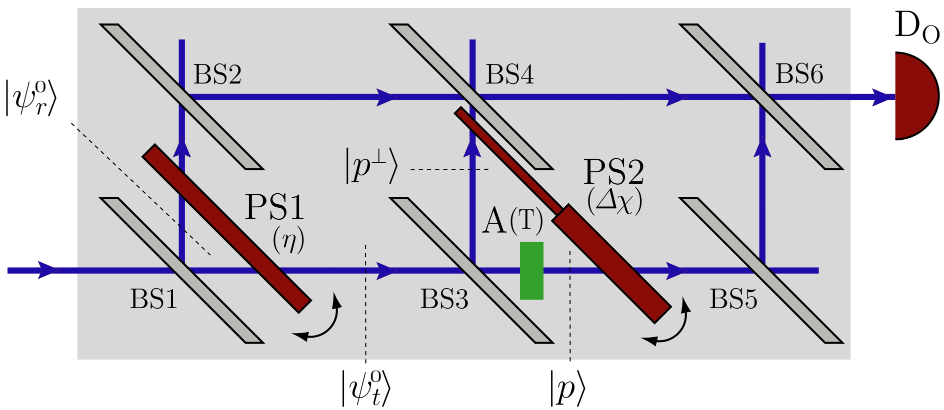

- 2-loop interferometer, unpolarized neutrons
- Geometric phase due to spatial degrees of freedom (2-level system)
- Phase Shifts $e^{i\chi_1}$, $e^{i\chi_2}$; Aborber (Transmission T)

- $I = \langle\psi_r'|\psi_r'\rangle + \langle\psi_{tf}'|\psi_{tf}'\rangle + 2|\langle\psi_r'|\psi_{tf}'\rangle|\cos(\eta - \arg\langle\psi_r'|\psi_{tf}'\rangle)$
- Parallel transport condition ($|\psi(\xi)\rangle = e^{-iCd_1\xi}|p^\perp\rangle + \sqrt{T}e^{iCd_2\xi}|p\rangle$):

$$\langle\psi(\xi)|\psi(\xi+\delta)\rangle \in \mathbb{R}$$

$$\rightarrow e^{-iCd_1\delta} + Te^{iCd_2\delta} = 0$$

$$\rightarrow \boxed{d_1 = Td_2 \qquad \Leftrightarrow \qquad \Phi_d = 0}$$

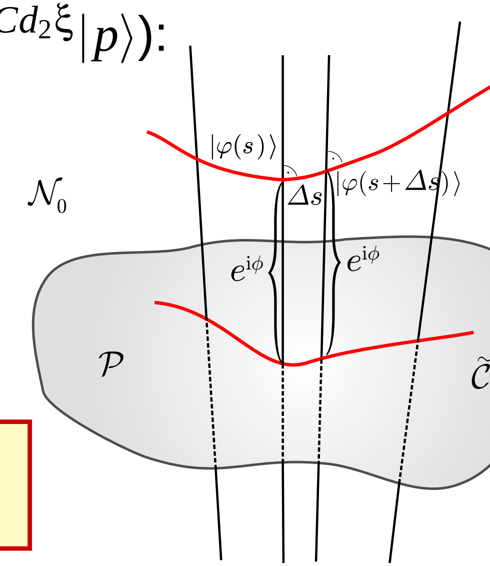

- $\boxed{\Phi_g = \arg\langle\psi_r'|\psi_{tf}'\rangle = \frac{\chi_1+\chi_2}{2} - \arctan\left[\tan\left(\frac{\chi_2-\chi_1}{2}\right)\left(\frac{1-\sqrt{T_2}}{1+\sqrt{T_2}}\right)\right]}$

ATOMINSTITUT FWF

Spatial geometric phase - Paths

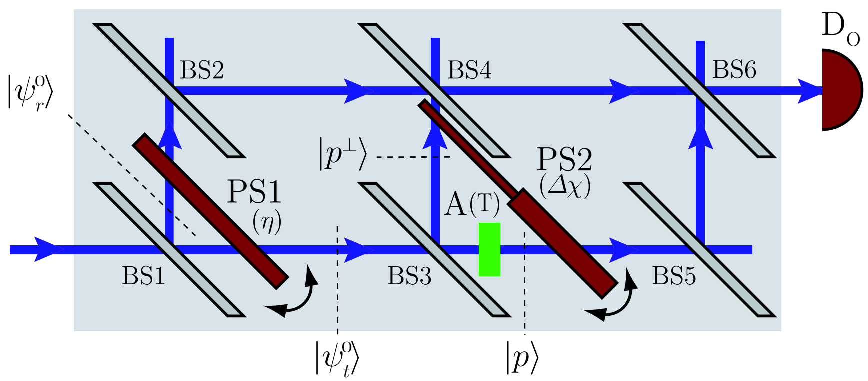

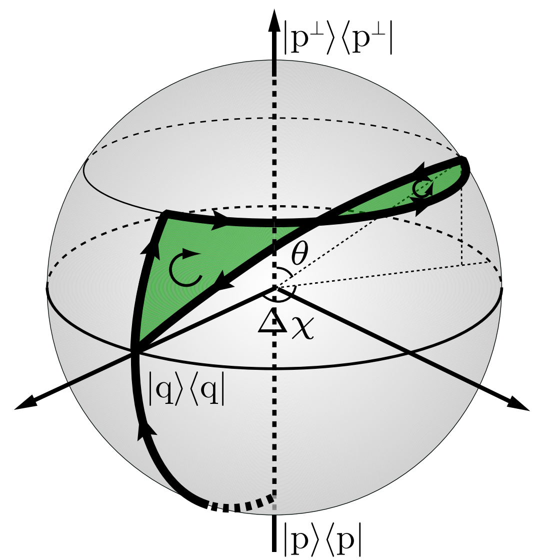

Superposition of Path 1 ($|p\rangle$) & Path 2 ($|p^\perp\rangle$ due to beamsplitter, absorber (T) and phase shifter ($\Delta\chi = \chi_2 - \chi_1$):

$$|\psi_{tf}\rangle \propto |p^\perp\rangle + e^{i\Delta\chi}\sqrt{T}|p\rangle$$

S. Filipp, Y. Hasegawa, R. Loidl, and H. Rauch. PRA **72** 021602(R) (2005) (eprint: quant-ph/0412038)

Spatial geometric phase - Paths

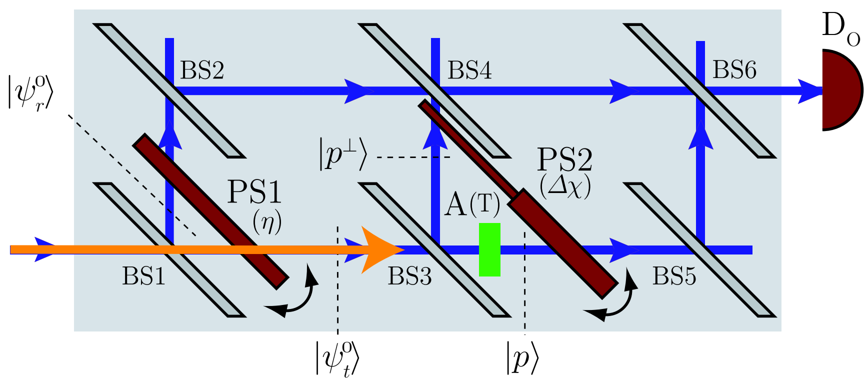

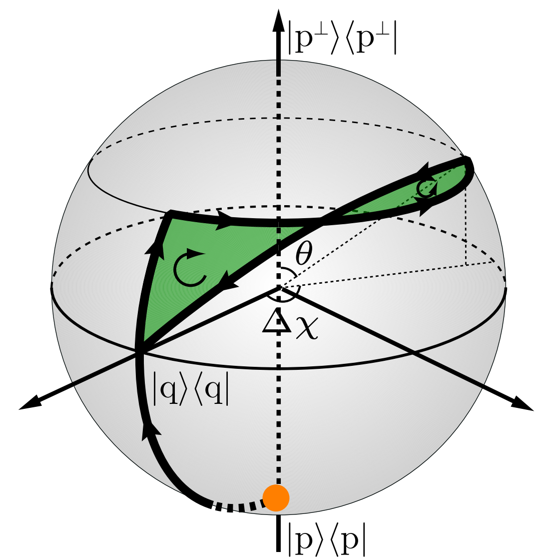

$$|\psi_t\rangle = |p\rangle \tag{1}$$

Spatial geometric phase - Paths

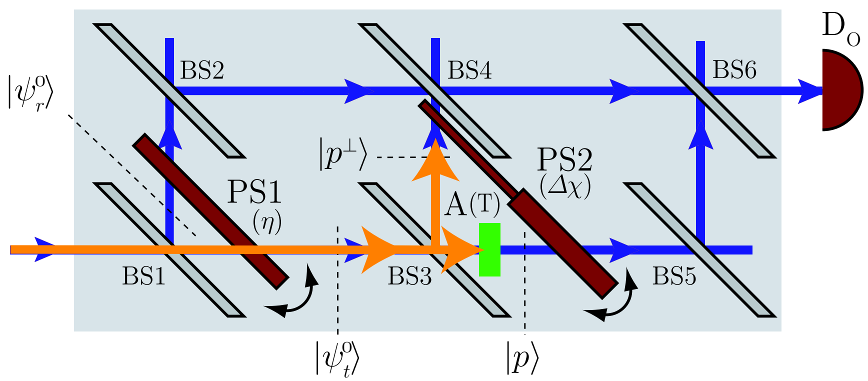

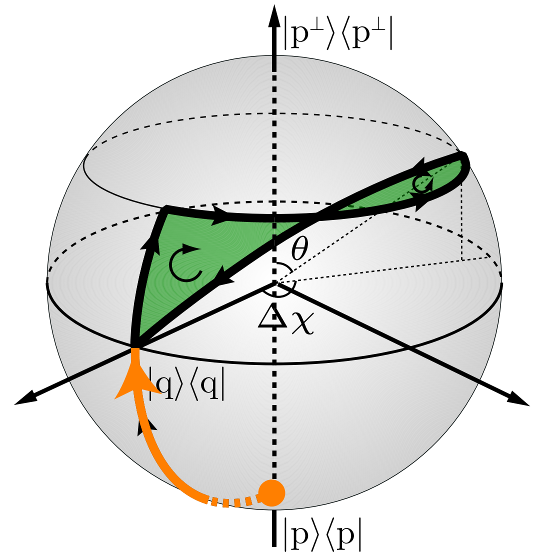

$$|\psi_t\rangle = \frac{1}{\sqrt{2}}(|p\rangle + |p^\perp\rangle) \qquad (2)$$

Spatial geometric phase - Paths

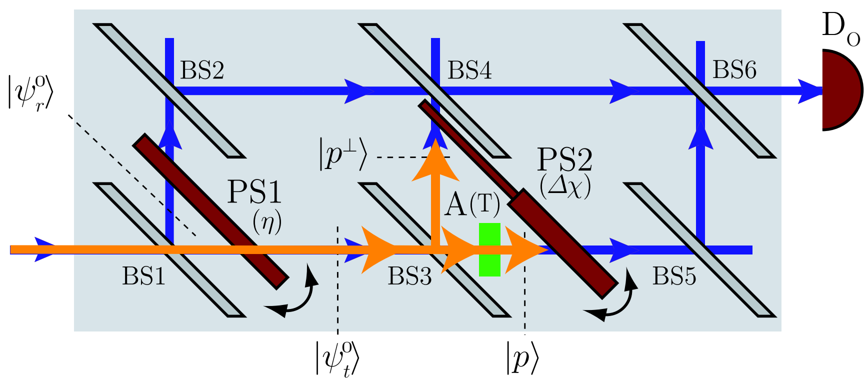

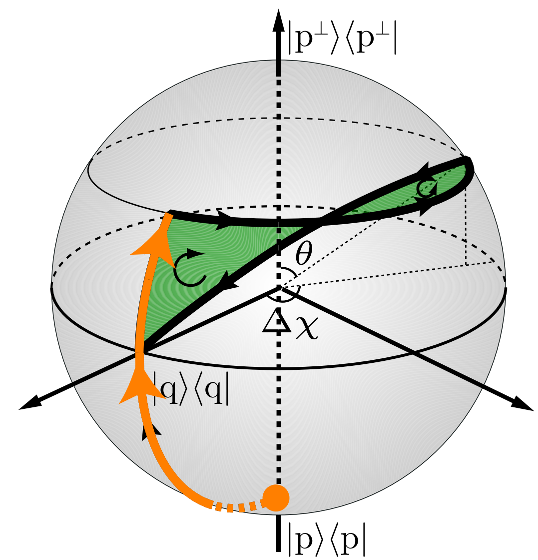

$$|\psi_t\rangle = \frac{1}{\sqrt{2}}(|p^\perp\rangle + \sqrt{T}|p\rangle) \tag{3}$$

Spatial geometric phase - Paths

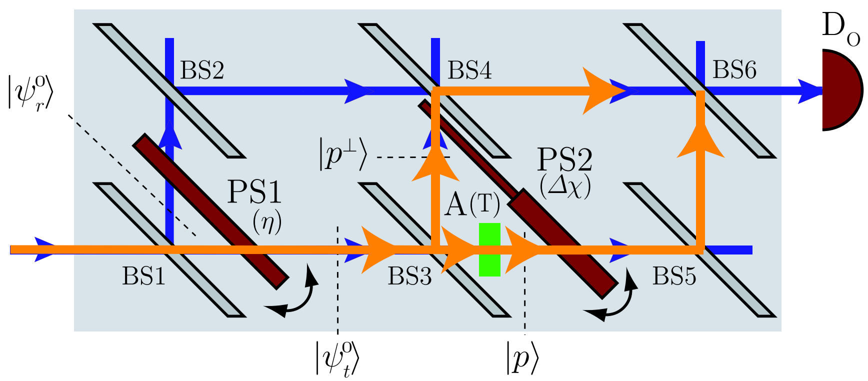

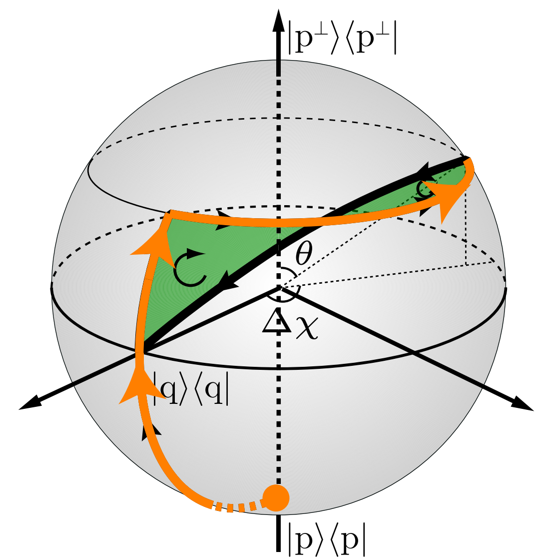

$$|\psi_{tf}\rangle = \frac{1}{\sqrt{2}}(|p^\perp\rangle + e^{i\Delta\chi}\sqrt{T}|p\rangle) \tag{4}$$

Spatial geometric phase - Paths

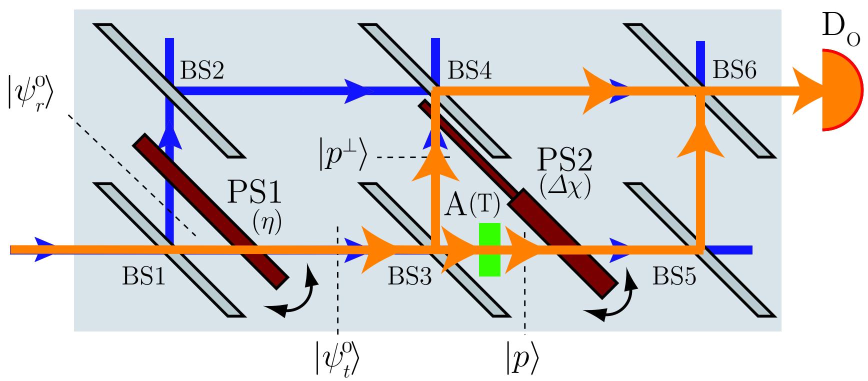

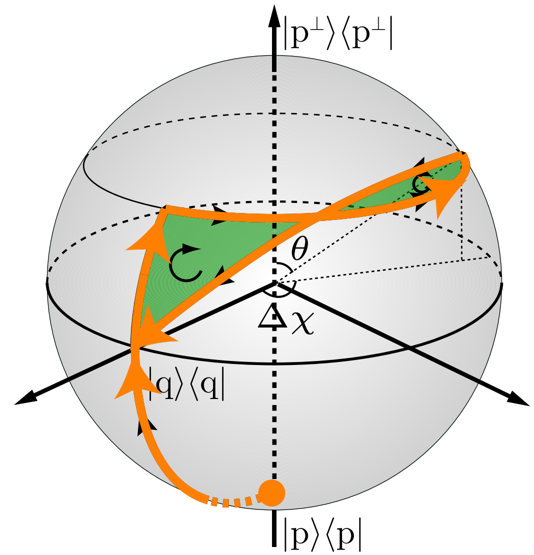

$$|\psi'_{tf}\rangle \propto (1+e^{i\Delta\chi}\sqrt{T})(|p\rangle+|p^\perp\rangle)$$

$$|\psi'_r\rangle \propto e^{i\Delta\chi}\sqrt{T}(|p\rangle+|p^\perp\rangle)$$

$$I = |e^{i\eta}|\psi'_r\rangle+|\psi'_{tf}\rangle|^2 = \langle\psi'_r|\psi'_r\rangle+\langle\psi'_{tf}|\psi'_{tf}\rangle+2|\langle\psi'_r|\psi_{tf'}\rangle|\cos(\eta-\arg\langle\psi'_r|\psi'_{tf}\rangle)$$

$$\boxed{\Phi = \arg\langle\psi'_r|\psi'_{tf}\rangle = \frac{\chi_1+\chi_2}{2} - \arctan\left[\tan\left(\frac{\Delta\chi}{2}\right)\left(\frac{1-\sqrt{T}}{1+\sqrt{T}}\right)\right]} \tag{5}$$

ATOMINSTITUT FWF

Results - 4.1mm/0.5mm & 4.1mm/4.1mm

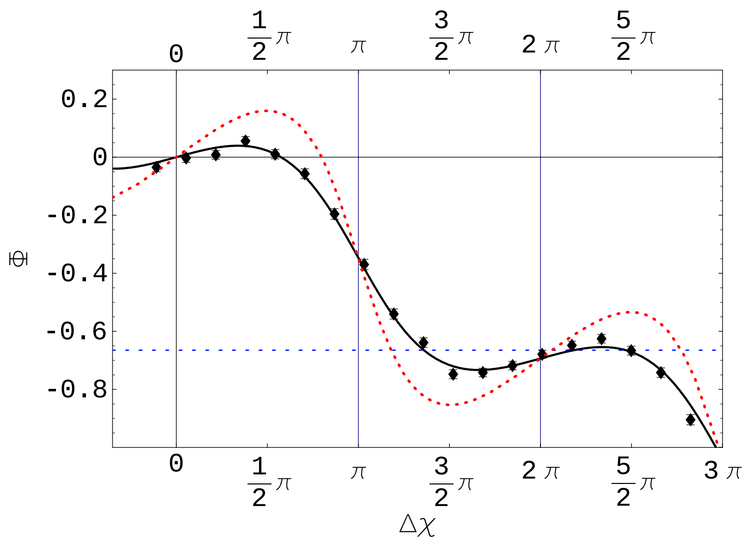

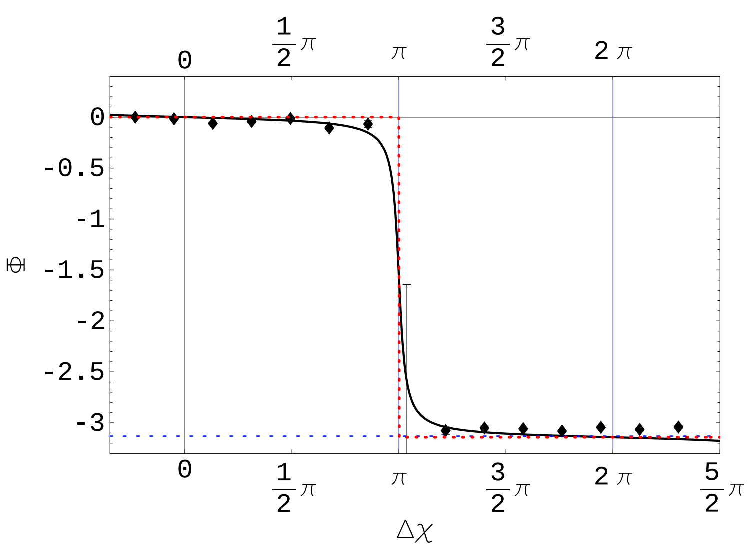

$\chi_1/\chi_2 = 4.1/0.5$:

$$\phi_g^{measured} = -0.665 \pm 0.010;\ \phi_g^{analytic} = -0.671$$

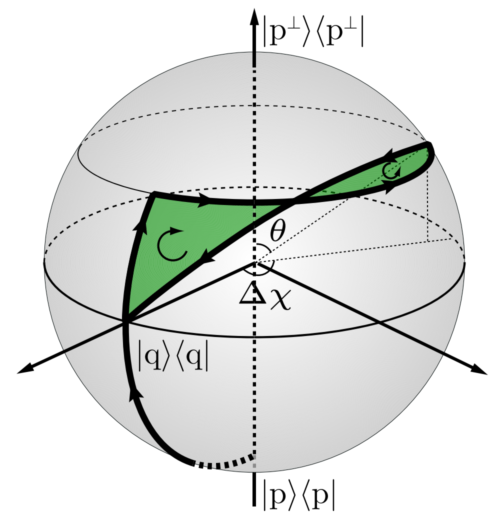

$\chi_1/\chi_2 = 4.1/4.1$:

$$\phi_g^{measured} = 3.113 \pm 0.017 \text{ rad}, \quad \phi_g^{analytic} = \pi$$

Mixed state phase - Polarimetry

J. Klepp, S. Sponar, Y. Hasegawa, E. Jericha, G. Badurek. PLA **342** 48 (2005).

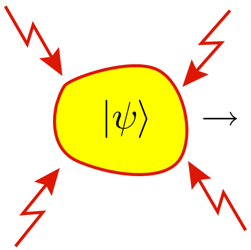

$$\rightarrow \varrho = \sum_i \frac{(1\text{-r}_i)}{2} |\psi_i\rangle\langle\psi_i|$$

$$\boxed{\phi_g \mapsto \phi_\rho \equiv \arg \mathrm{Tr}[U\rho] = \arg \sum_i p_i \langle\psi_i|U|\psi_i\rangle}$$

Mixed state phase - Polarimetry

J. Klepp, S. Sponar, Y. Hasegawa, E. Jericha, G. Badurek. PLA **342** 48 (2005).

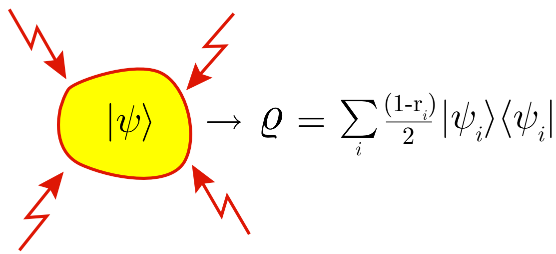

$$\boxed{\phi_g \mapsto \phi_\rho \equiv \arg \mathrm{Tr}[U\rho] = \arg \sum_i p_i \langle\psi_i|U|\psi_i\rangle}$$

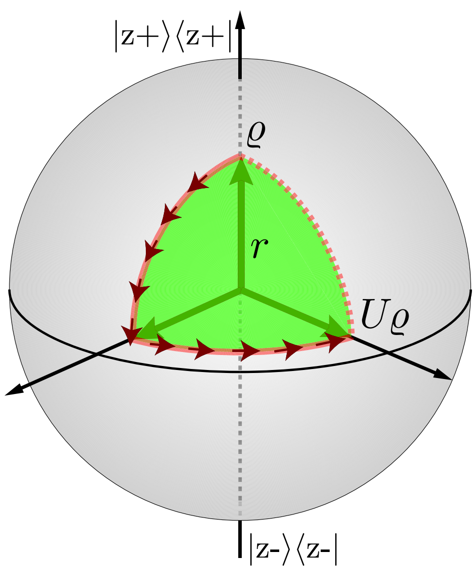

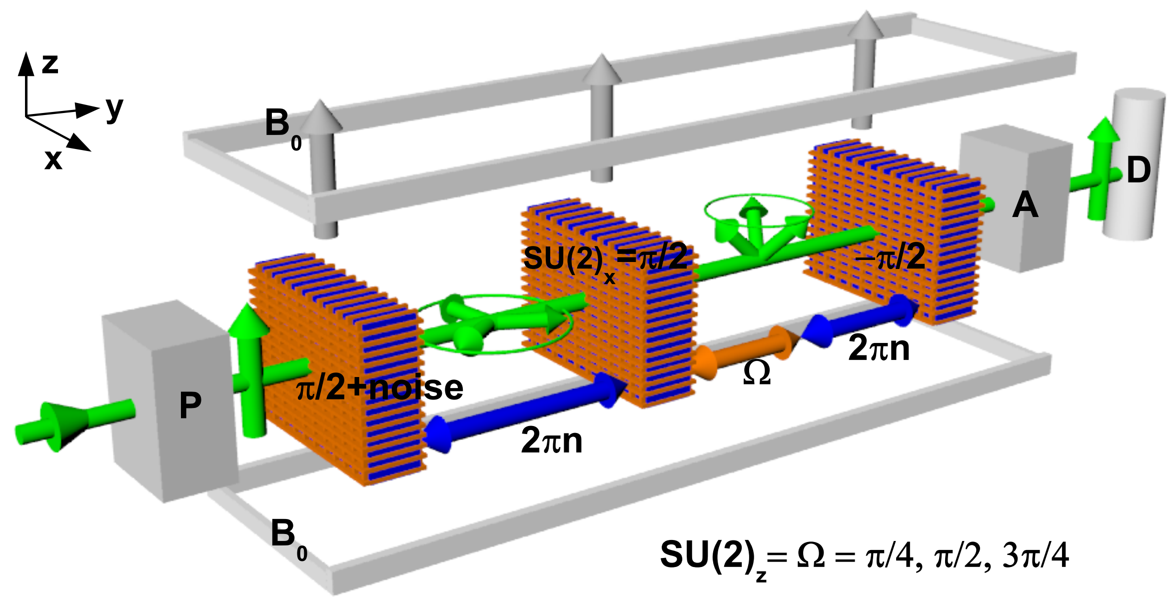

Larsson and Sjöqvist, PLA **315** 12 (2003)

Production of mixed states

Electronic Random Noise fluctuations produces dephasing.

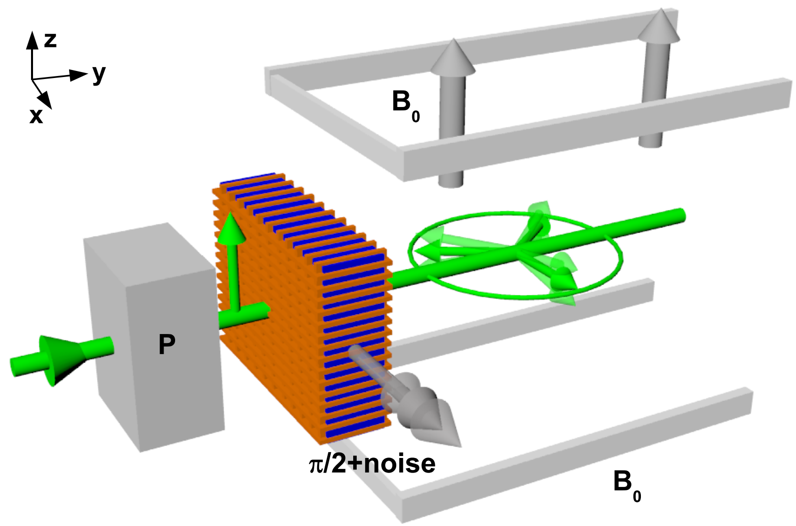

Results

Mixed state phase ϕ_ρ:

$$\boxed{\phi_\rho = \arccos\sqrt{\frac{I_{min}-(1-r)/2}{I_{min}-(1-r)/2+r^2\left((1+r)/2-I_{max}\right)}}}$$

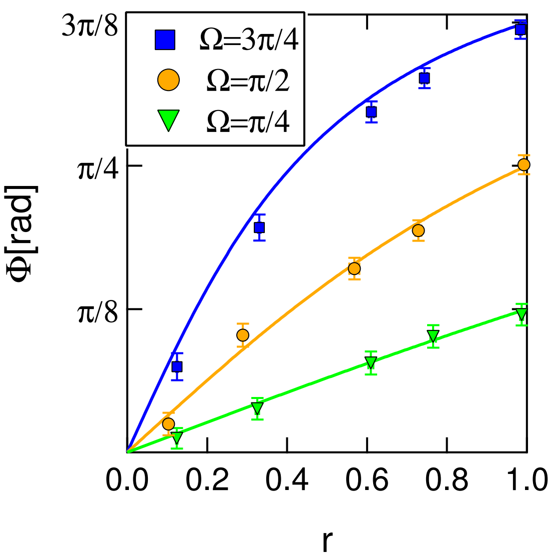

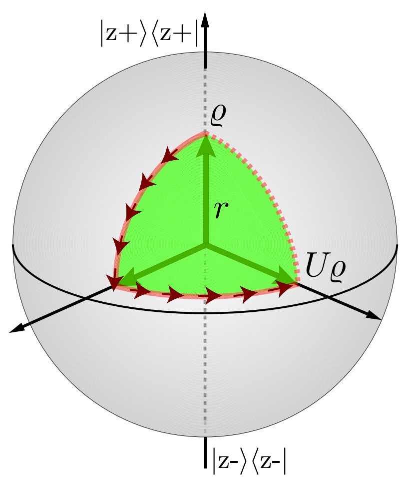

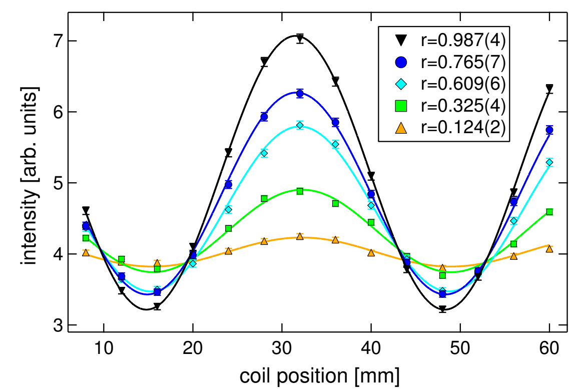

J. Klepp, S. Sponar, Y. Hasegawa (in preparation).

ATOMINSTITUT FWF

Dephasing...

Noise in one interferometer arm leads to dephasing.

[M. Baron, H. Rauch and M. Suda, J. Opt. B **5**, 5241 (2003).]

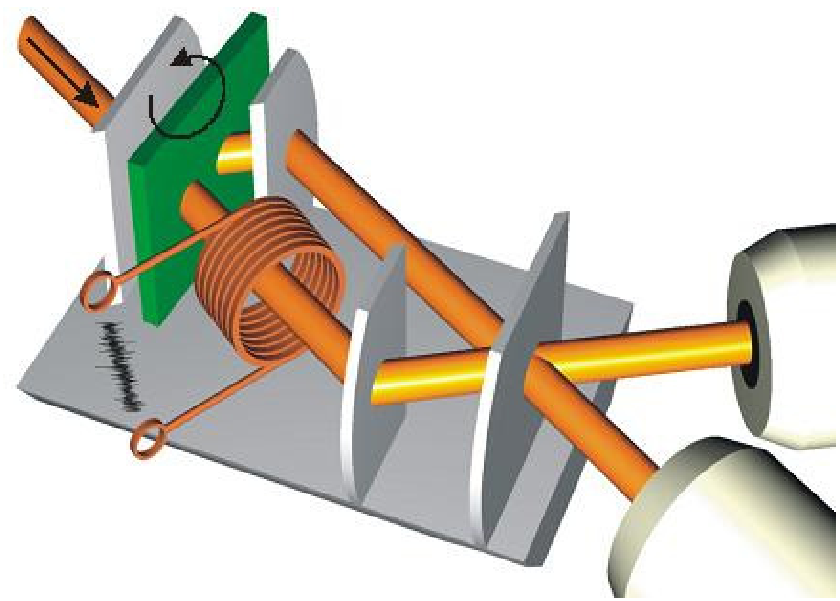

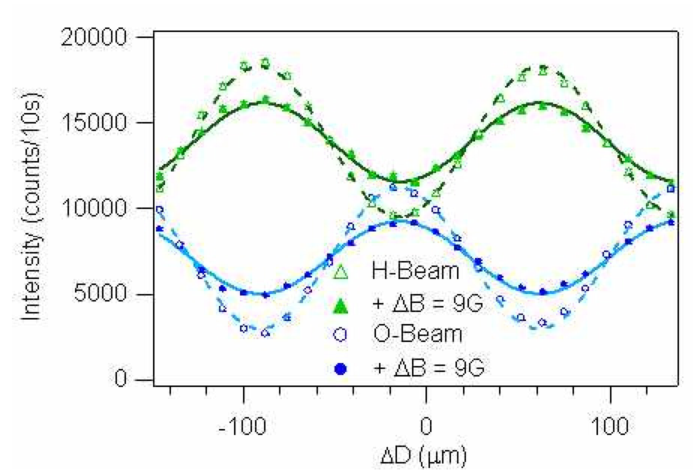

... and how to fight it

By applying equal magnetic fields in both arms interference fringes can be retrieved.

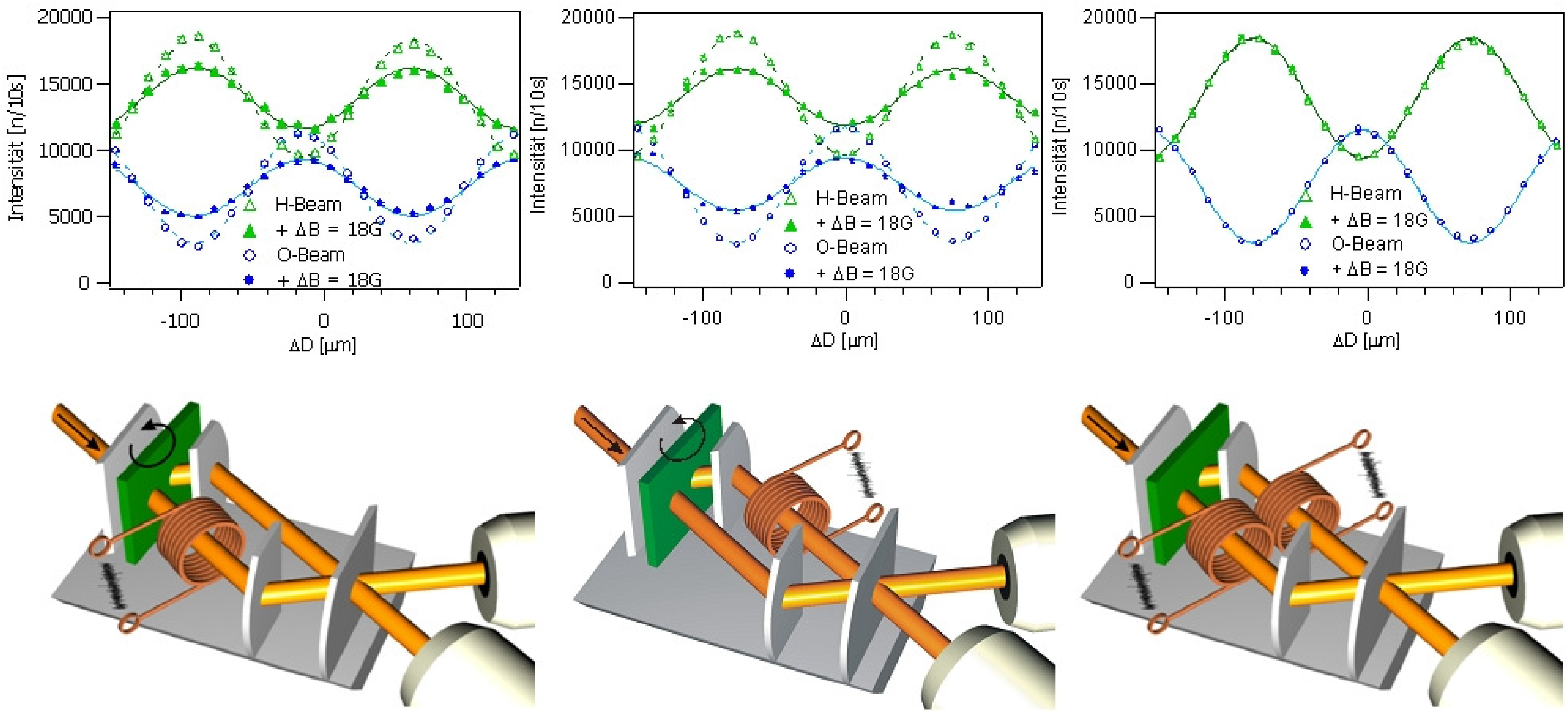

Geometric dephasing

DeChiara and Palma [PRL **91, 090404 (2003)**]**:**

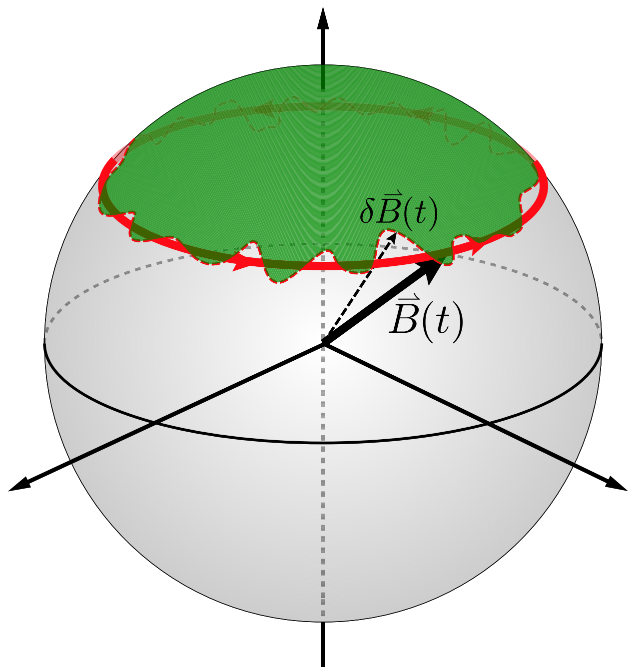

- Adiabatic evolution with small fluctuations of the direction of the magnetic field
- Perturbations in the magnetic field induce deviations in phase, but ϕ_g is stabilizing for increasing time
- Basic ingredients:
  Spin-1/2 particles (neutrons) + controllable 3D- magnetic field.

Numerics

Variance of geometric phase vanishes for long evolution time:

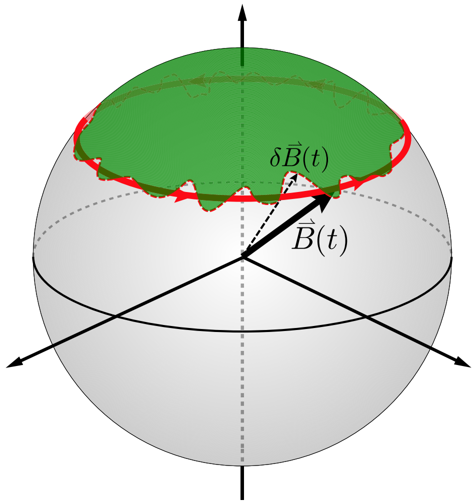

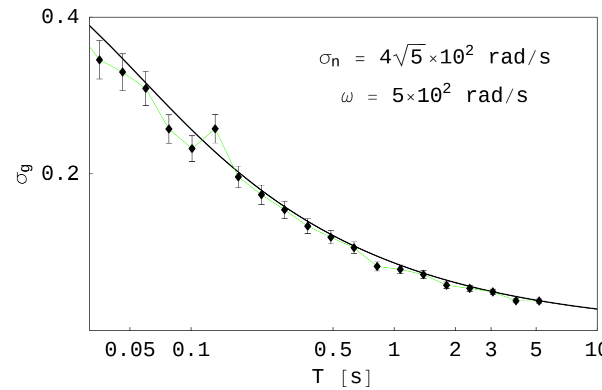

Numerics

Variance of geometric phase vanishes for long evolution time:

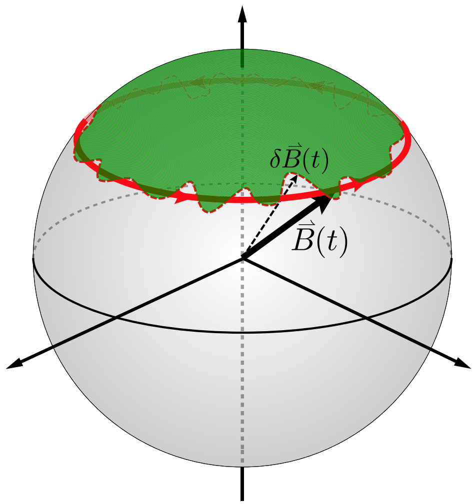

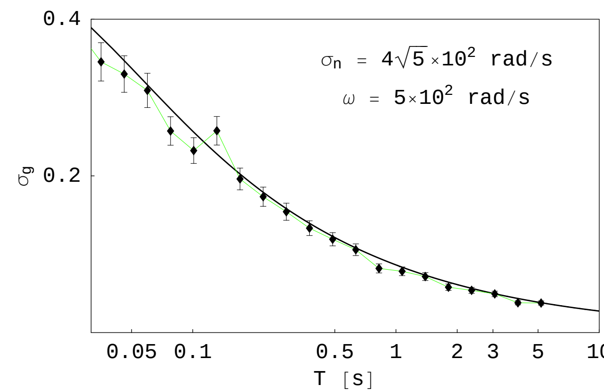

Mean Geometric Phase $\overline{\phi}_g$ equal to noisefree geometric phase (1^{st} order). But:

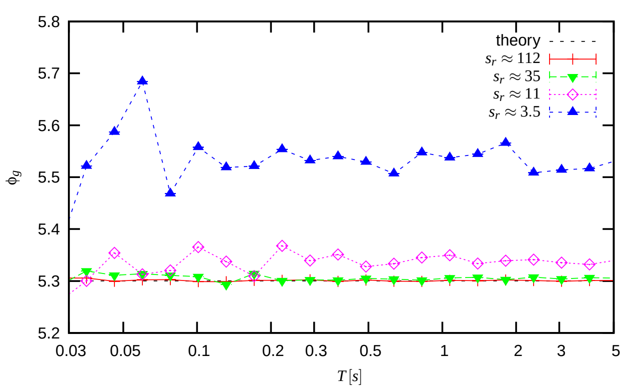

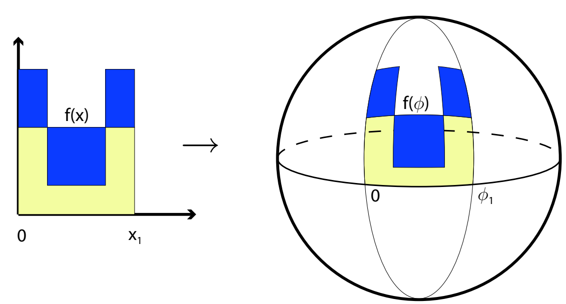

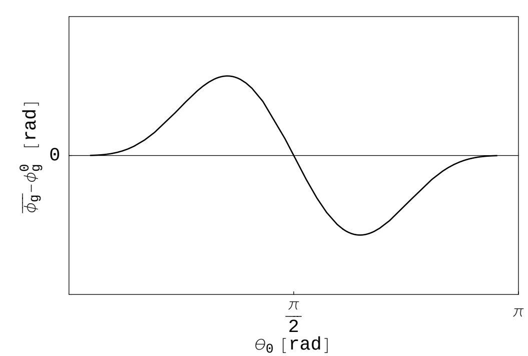

Setup

PF2, ILL, Grenoble:

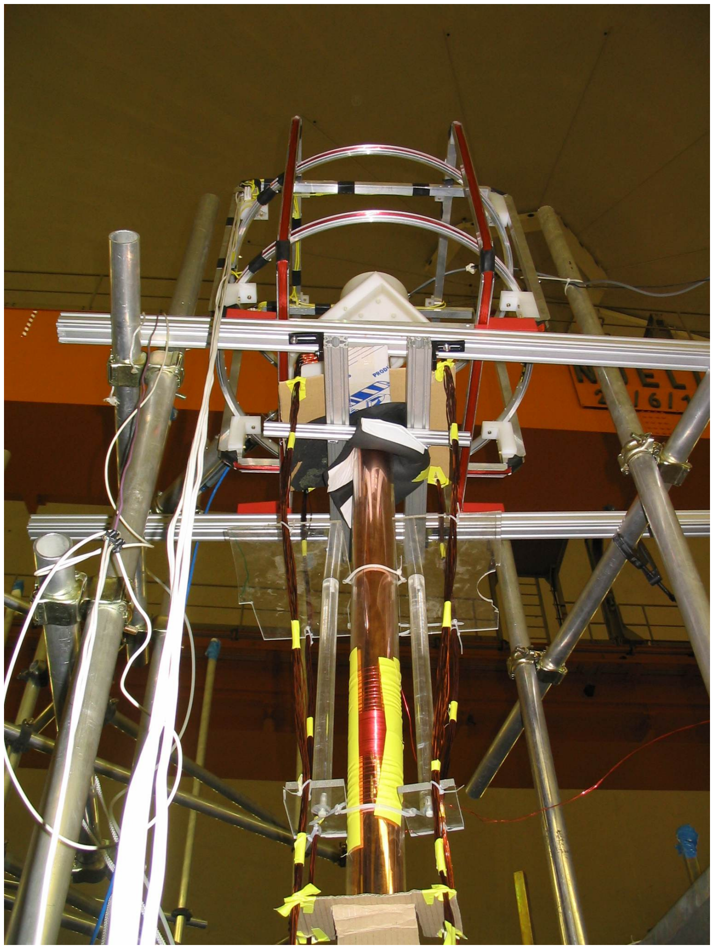

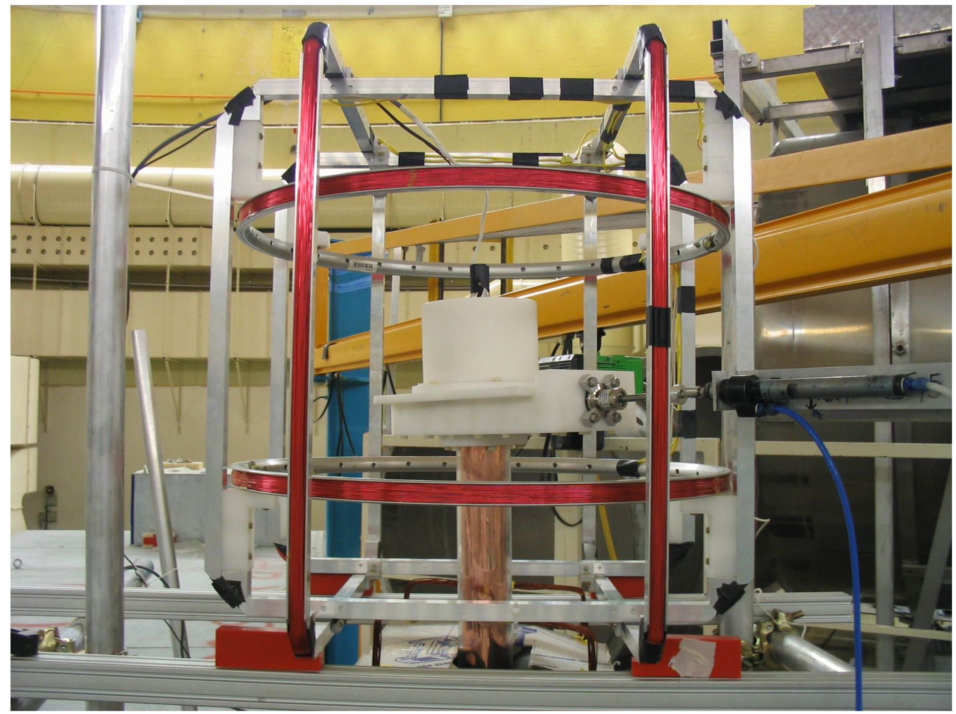

Spin superposition

Ramsey - Fringes:
(Guide-Field: 89 mG, ω = 1829(10) rad/s)

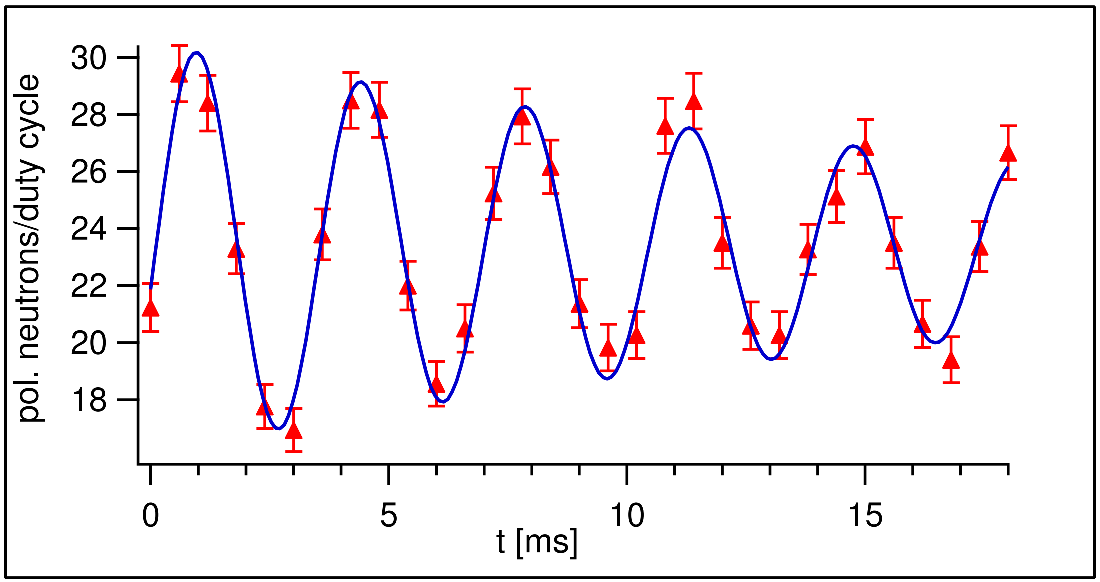

Decoherence still too dominant ($T_2 = 20(5)$ ms)!

Spin-Path Entanglement

Photons

2-particle entanglement

$$|\Psi\rangle = \frac{1}{\sqrt{2}}\left(|H\rangle_1 \otimes |V\rangle_2 + |V\rangle_1 \otimes |H\rangle_2\right)$$

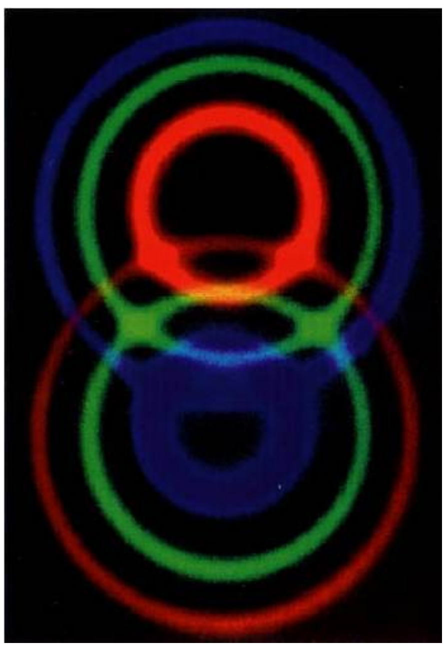

photo: Kwiat and Reck

Spin-Path Entanglement

Photons

2-particle entanglement

$$|\Psi\rangle = \frac{1}{\sqrt{2}}\left(|H\rangle_1 \otimes |V\rangle_2 + |V\rangle_1 \otimes |H\rangle_2\right)$$

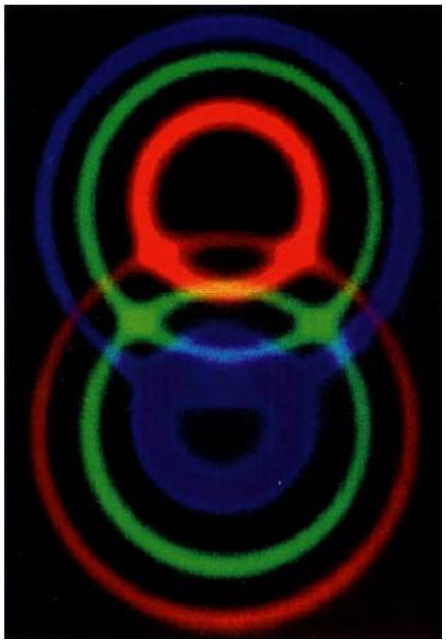

photo: Kwiat and Reck

Neutrons

single particle spin-path entanglement,

paths in interferometer analogous to 2nd particle

$$|\Psi\rangle = \frac{1}{\sqrt{2}}\left(|\uparrow\rangle \otimes |I\rangle + |\downarrow\rangle \otimes |II\rangle\right)$$

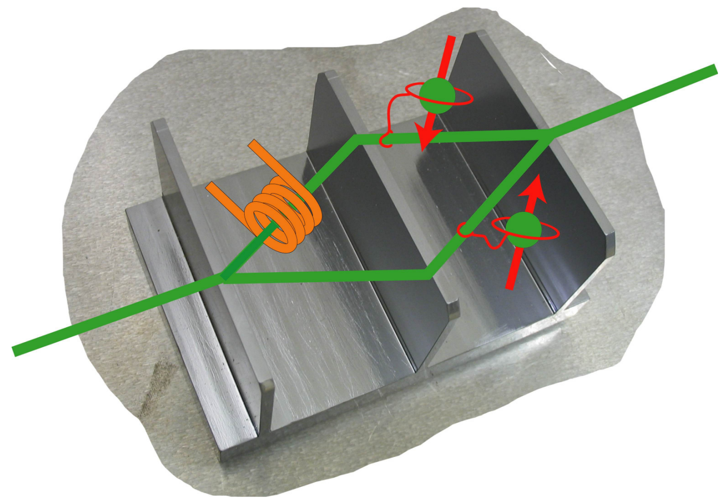

State Tomography

Matrix-representation of Bell state $|\Psi^+\rangle = \frac{1}{\sqrt{2}}(|\uparrow\rangle \otimes |I\rangle + |\downarrow\rangle \otimes |II\rangle)$

$$|\Psi^+\rangle\langle\Psi^+| = \frac{1}{2}\begin{pmatrix} 1 & 0 & 0 & 1 \\ 0 & 0 & 0 & 0 \\ 0 & 0 & 0 & 0 \\ 1 & 0 & 0 & 1 \end{pmatrix}$$

Basis: $\{|\uparrow\rangle|I\rangle, |\uparrow\rangle|II\rangle, |\downarrow\rangle|I\rangle, |\downarrow\rangle|I\rangle\}$

In general, a (not normalized) bipartite state is determined by 16 parameters

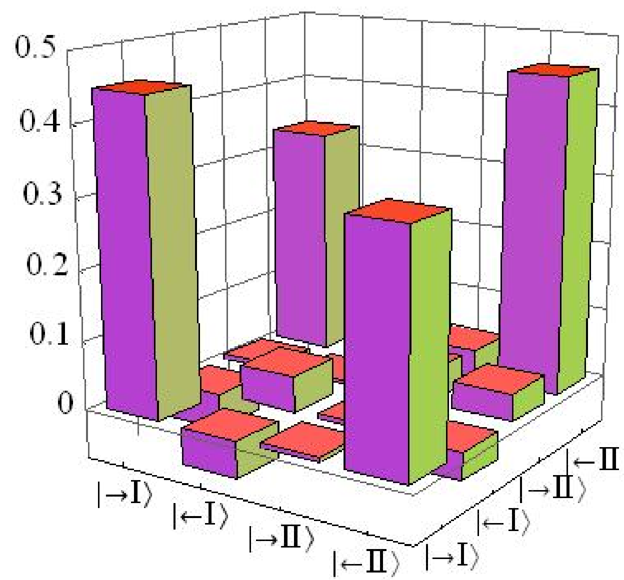

Measurement Scheme

Observables: Projective Measurements $P_a = 1/2(1 + |a\rangle\langle a|)$

Path: $\begin{cases} \chi = 0, \frac{\pi}{2} & P^p_{+x}, P^p_{+y} \\ \text{beamblock I,II} & P^p_{+z}, P^p_{-z} \end{cases}$

Spin: $\begin{cases} \alpha = 0, \pi & P^s_{+z}, P^s_{-z} \\ \alpha = \pi/2 & P^s_{+x}, P^s_{+y} \end{cases}$

Example:

$< P^p_{+x} P^s_{\pm z} >, < P^p_{+y} P^s_{\pm z} >$

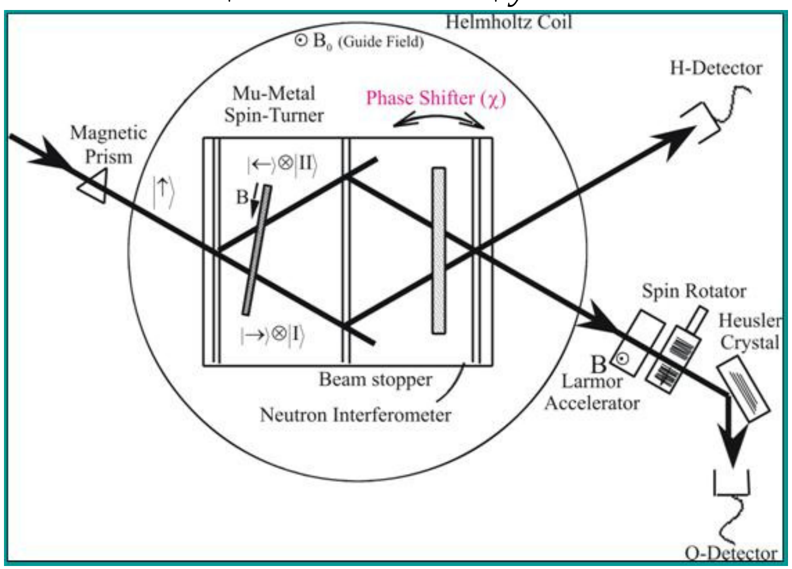

$< P^p_{\pm z} P^s_{+x} >, < P^p_{\pm z} P^s_{\pm z} >$

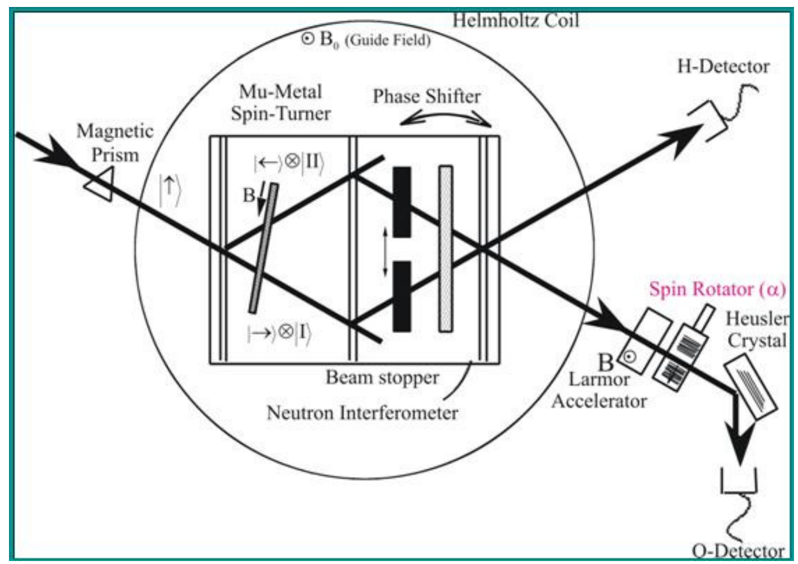

$\rightarrow$ 16 combinations

Measurement Schemes

Three different states:

1. $|\Psi_1\rangle = |+x\rangle|I\rangle + |-x\rangle|II\rangle$
2. $|\Psi_2\rangle = |-x\rangle|I\rangle + |+x\rangle|II\rangle$
3. $|\Psi_3\rangle = |+x\rangle(|I\rangle + |II\rangle)$

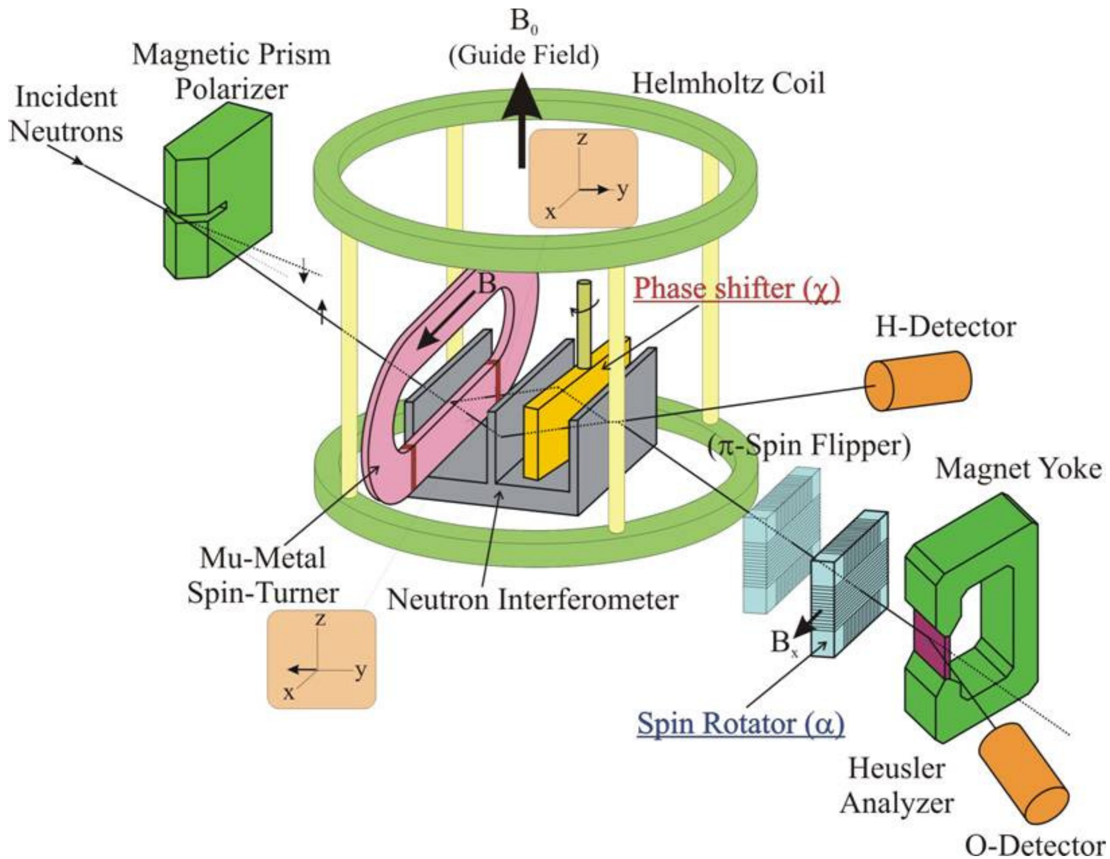

Results

$$|\Psi_1\rangle = |+x\rangle|I\rangle + |-x\rangle|II\rangle \qquad |\Psi_2\rangle = |-x\rangle|I\rangle + |+x\rangle|II\rangle \qquad |\Psi_3\rangle = |+x\rangle(|I\rangle + |II\rangle)$$

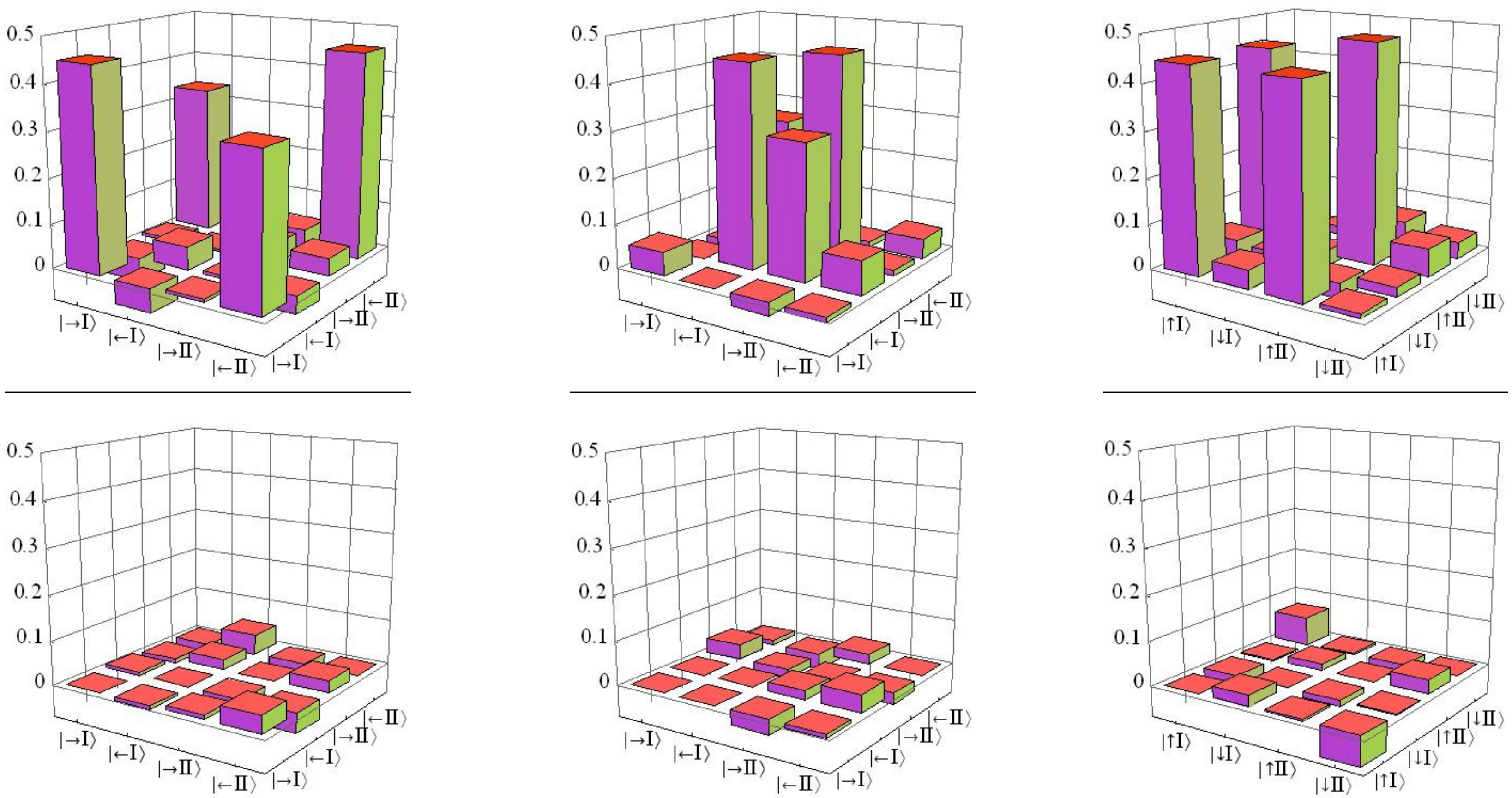

F=0.785 F=0.749 F=0.908

Y. Hasegawa, J. Klepp, S. Filipp, R. Loidl and H. Rauch (in preparation).

Bell Inequalities

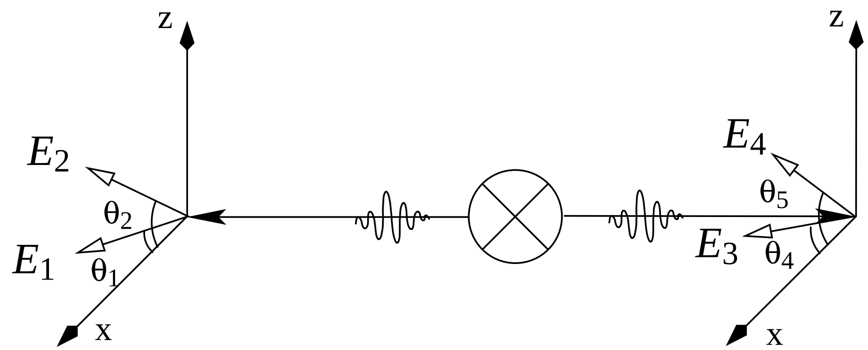

- Entanglement leads to violation of Bell-type Inequality
- $\rightarrow$ spin-path entangled state also violates a Bell Inequality

CHSH- Inequality: $\boxed{-2 < S = \mathcal{E}(E_1,E_3)+\mathcal{E}(E_1,E_4)+\mathcal{E}(E_2,E_3)-\mathcal{E}(E_2,E_4) < 2}$

$$\mathcal{E}(E_i,E_j) = \langle\Psi|(n_i\sigma)\otimes(n_j\sigma)|\Psi\rangle = \frac{N_{ij}(+,+)+N_{ij}(-,-)-N_{ij}(+,-)-N_{ij}(-,+)}{\sum N_{ij}(\pm,\pm)}$$

$$N_{ij}(\pm,\pm) = \langle\Psi|P_i^s\otimes P_j^p|\Psi\rangle$$

Bell Inequality - Observables

- *Photons:* Polarization of particle 1 and 2 along $n_{1,2}$-axis
- *Neutrons:* Spin-polarization along n-axis and “which-path” by rotation of phase shifter
- Quantum Mechanics predicts non-local/contextual correlations

$$\boxed{S_{\mathrm{max}} = 2\sqrt{2}} \text{ (Tsirelson Bound)}$$

Measurements

Path: Spin:

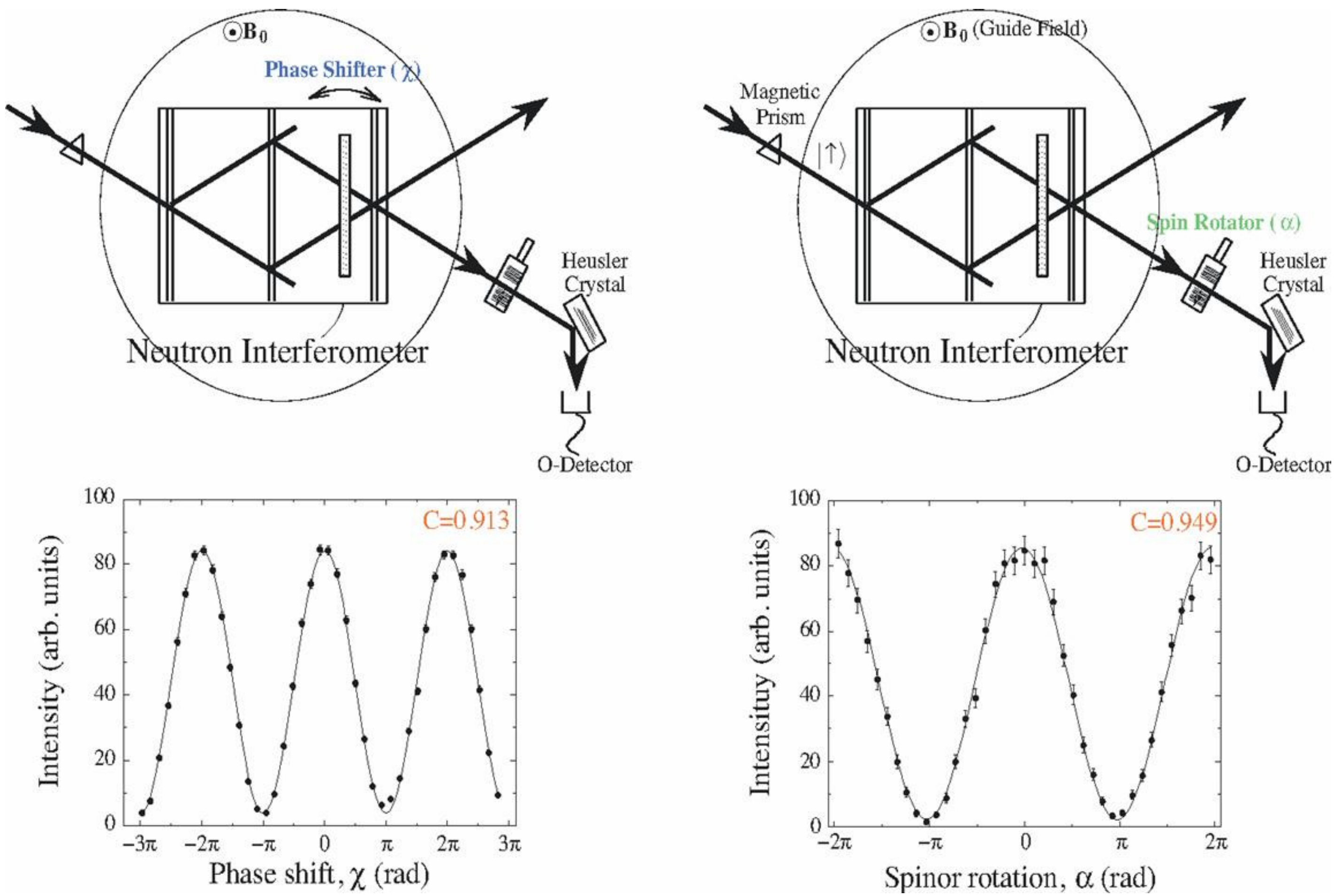

Violation of BI with Neutrons

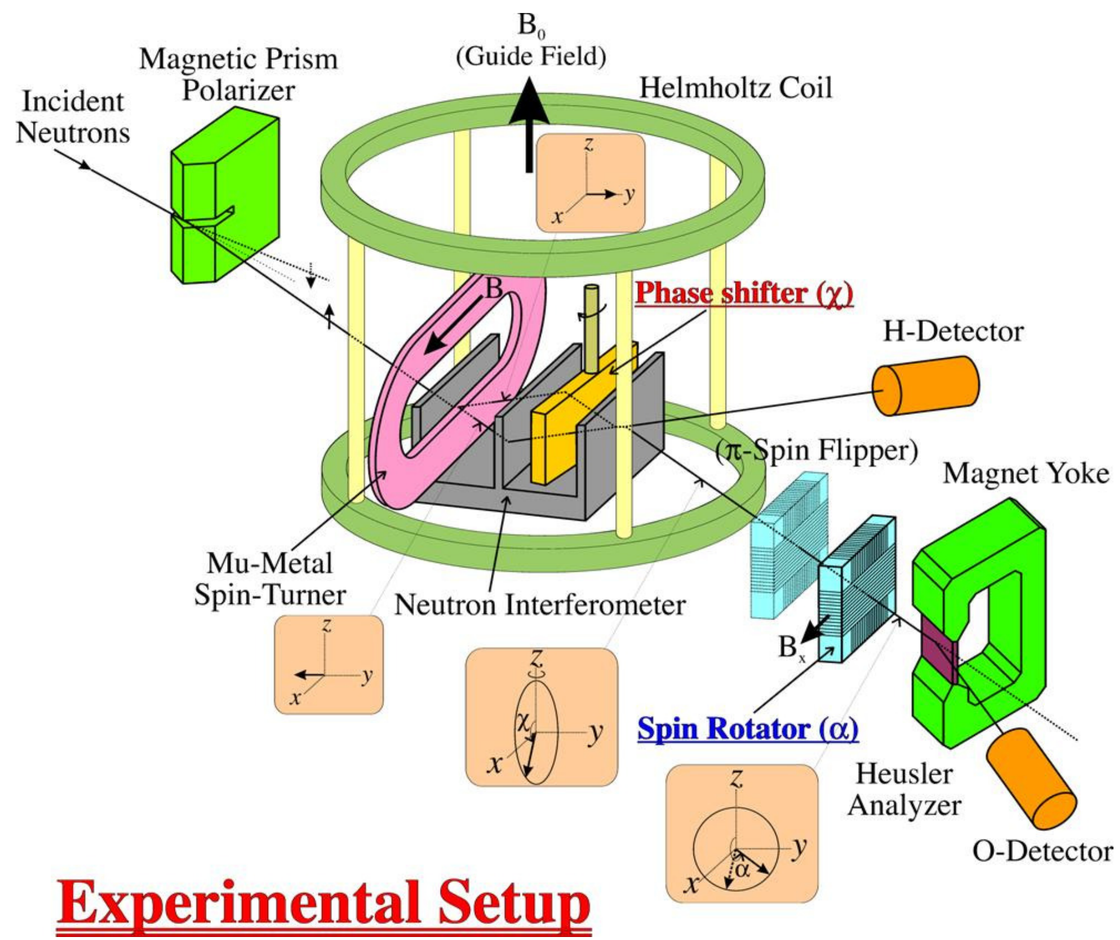

$$\boxed{S = 2.051 \pm 0.019}$$

Hasegawa, Loidl, Badurek, Baron and Rauch. Nature **425** (2003) 45.

Summary and Outlook

- Measurement of phases with different neutron interferometry techniques:
  - Interferometer: Confinement induced phase shift, Spinor geometric phase, Spatial geometric phase, Dephasing
  - Polarimeter: Mixed state geometric phase
  - UCNMR: Dephasing of the geometric phase
- Spin-Path entanglement
  - State tomography
  - Bell inequality test
- Forthcoming experiments:
  - Dephasing of the geometric phase
  - Geometric phase and entanglement
  - Quantum Contextuality - Kochen-Specker-like contradictions
  - Irreversibility
  - Phase of non-unitary transformation

ATOMINSTITUT FWF